SAND2022-9678C

Molecular Modeling of Smectites and Interaction of Various Molecules with their Surfaces

Andrey G. Kalinichev[1], Jeffery A. Greathouse[2], Randall T. Cygan[2]

[1] Laboratoire SUBATECH (UMR 6457– IMT Atlantique, Nantes Université, CNRS), Nantes, France

[2] Geochemistry Department, Sandia National Laboratories, Albuquerque, NM, USA

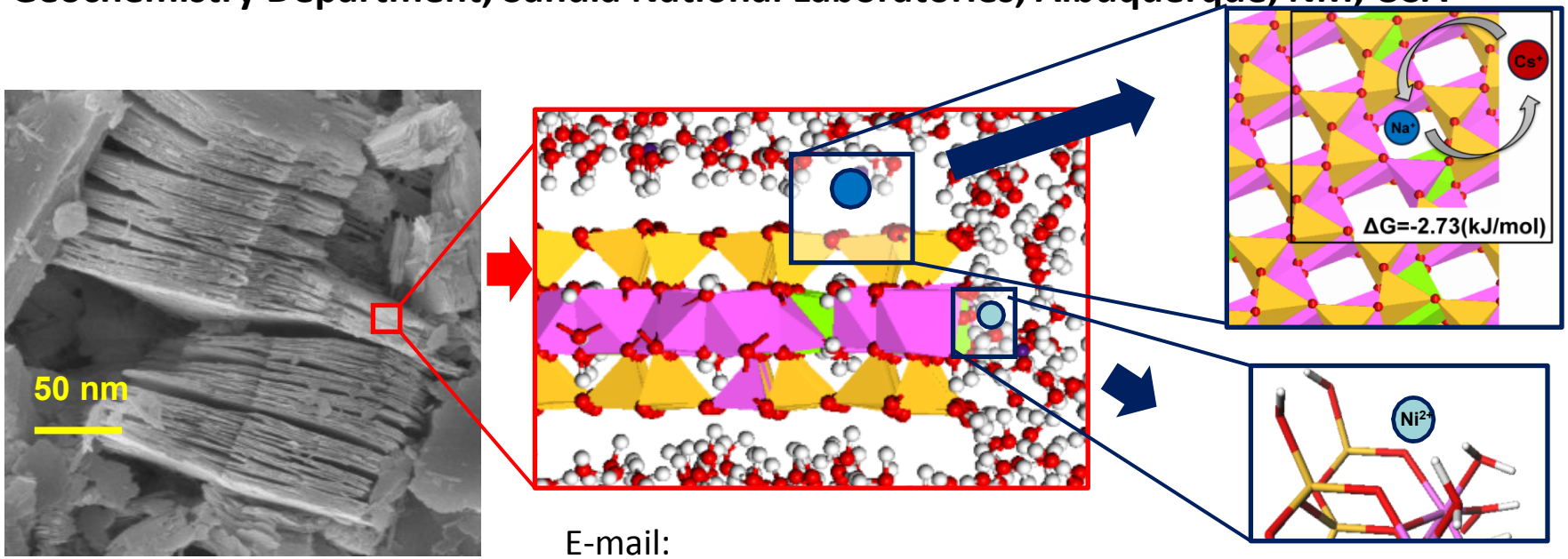

E-mail:
kalinich@subatech.in2p3.fr

Time and Length Scales of Materials' Simulation

- Continuum mechanics
- Macroscopic thermodynamics
- Reactive transport

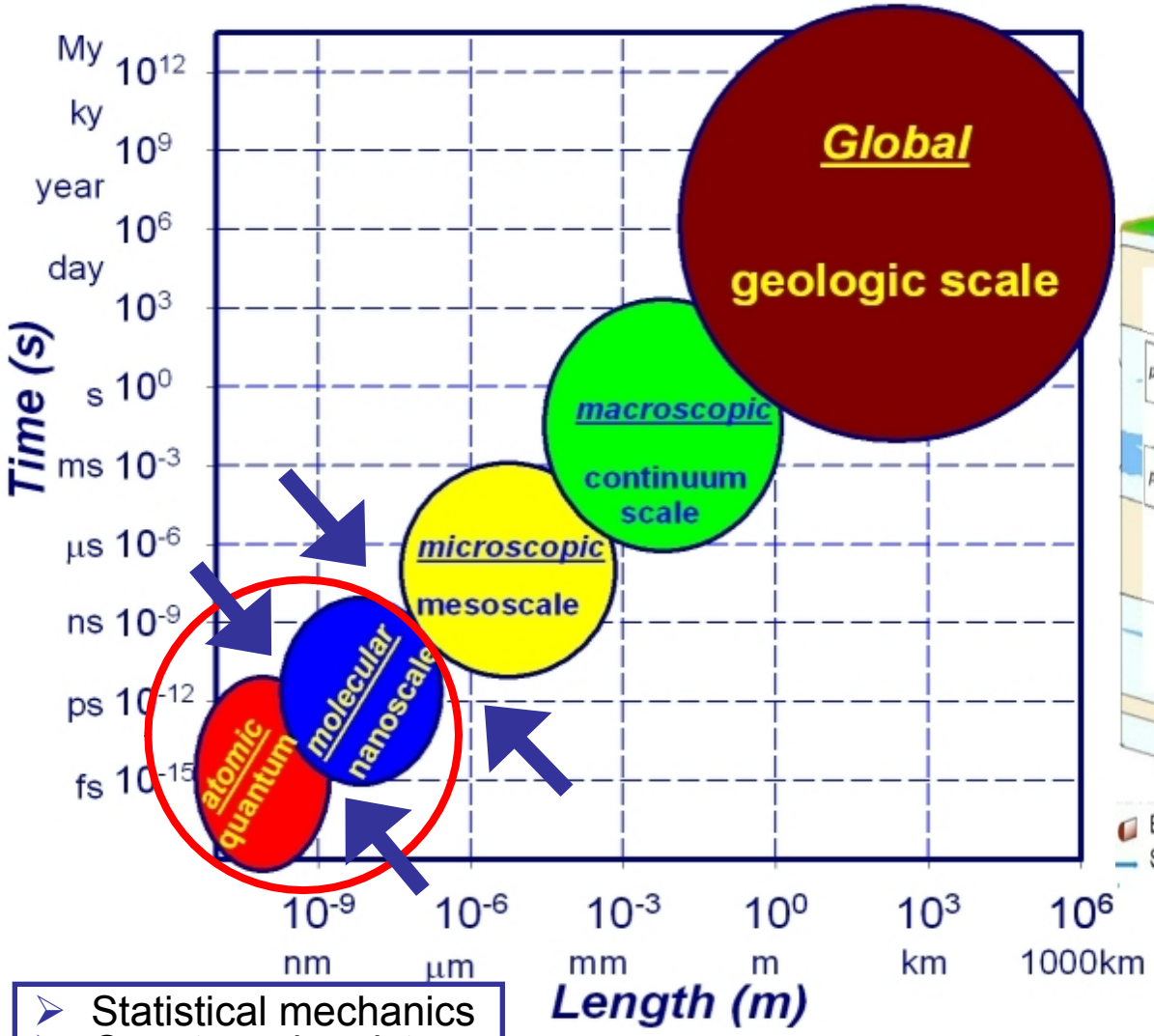

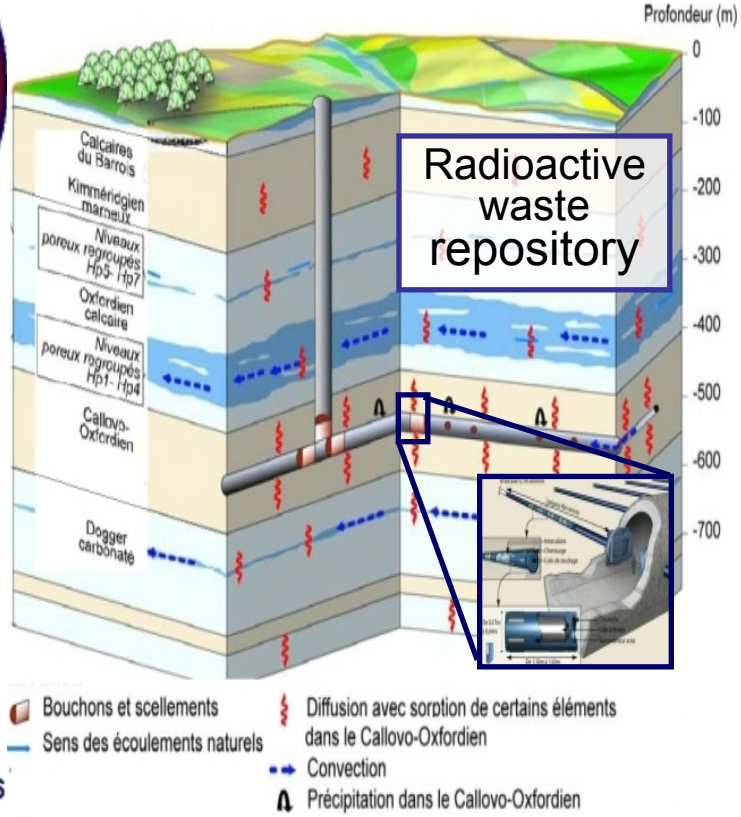

- Statistical mechanics
- Quantum chemistry

Molecular-Scale View of Reactive Hydrated Smectite Interfaces

- Most geochemical reactions take place at ***mineral-solution interfaces***
- Mineral ***weathering*** processes
- Adsorption or release of ***contaminants*** and nutrients ***in soil and water***
- ***Drinking water*** **quality**
- ***Shale oil and gas exploration***

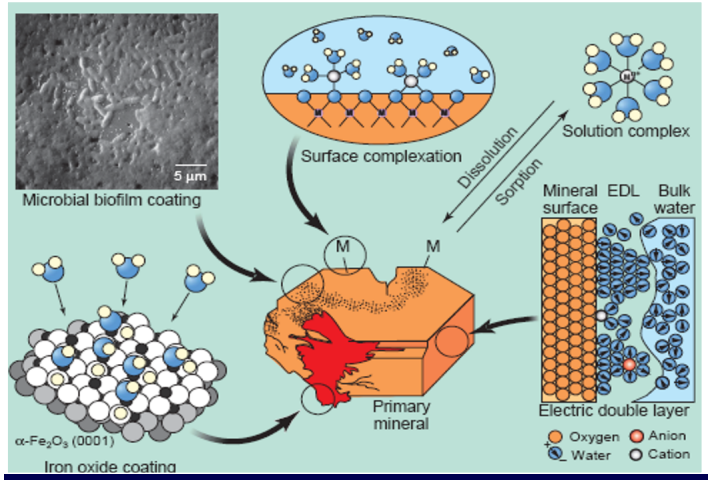

G. Brown, *Science* **294**, 67-70 (2001)

- Fate of CO_2 in ***geologic carbon sequestration***
- Formation and behavior of ***ice nano-crystals*** and hydrated mineral nano-particles ***in the atmosphere***
- Geochemical mechanisms of primitive metabolism and the ***origin of life***
- Bentonites for ***geological disposal of radioactive waste***

Molecular scale is, in fact, ***inherently multi-scale*** in time and distance

Structure
Dynamics
Reactivity

at hydrated mineral interfaces are ***inherently coupled with each other***, and none of them can be adequately understood without the others

Molecular-Scale View of Confined Fluids and Interfaces

- Recent progress of the surface-sensitive experiments
  - ✓ Synchrotron X-ray reflectivity, EXAFS
  - ✓ Inelastic and quasielastic neutron scattering
  - ✓ Sum-frequency vibrational spectroscopy (SFVS)
  - ✓ Multi-nuclear multi-dimensional NMR spectroscopy
- Probe the properties of H_2O molecules and aqueous species at mineral surfaces or in nano-confinement, provide direct molecular-scale information on the structure and dynamics of hydrated interfaces
- However, these complex experimental data are often difficult to interpret unambiguously

Molecular computer simulations can provide a complementary powerful quantitative tool to facilitate the atomic-scale interpretation of the observed interfacial phenomena, the effects of substrate structure and composition on the structure, dynamics, and composition of the interfacial aqueous solution

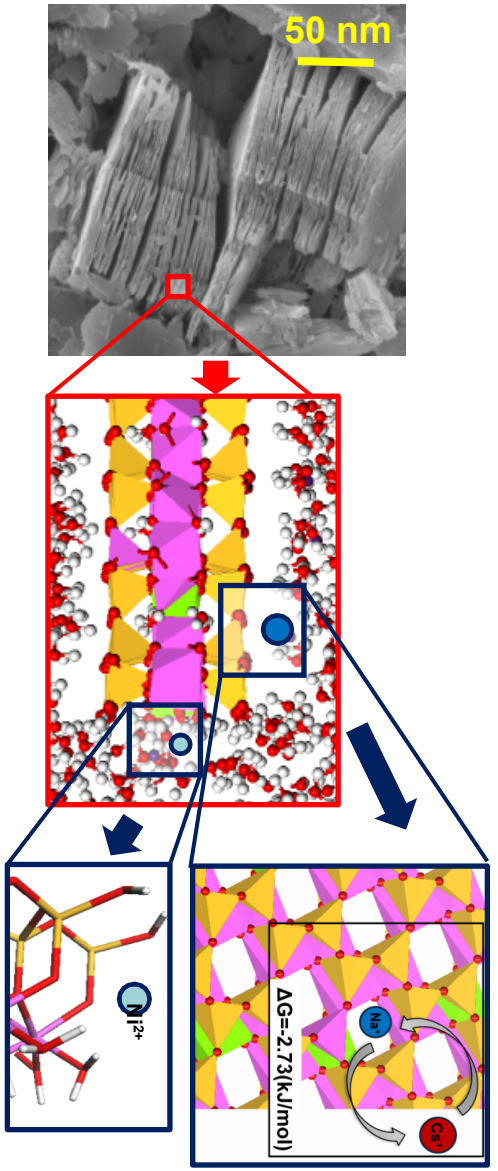

Computational Atomistic Modeling: Tools and Objectives

- ***Molecular Dynamics (MD)*** - deterministic approach
- ***Monte Carlo (MC)*** - stochastic approach
- In both approaches, MD or MC, the formalism of ***statistical mechanics*** is used to develop quantitative molecular-level understanding of the complex behavior of clays and clay-related materials and interfaces:
  - ✓ Structure and dynamics of aqueous and interfacial species
  - ✓ Hydration, adsorption, complexation, diffusion, intercalation, H-bonding
  - ✓ Atomistic mechanisms of ionic sorption and transport

L ~ 10-100 nm $N \sim 10^3$-10^6 $n \sim 10^7$-10^9 conf.

$\Delta t \sim 1$ fs $= 10^{-15}$ s $\tau \sim$ 1-10 ns $\sim 10^6$-$10^7 \Delta t$

need significant computing power, **but**

Atomistic computational modeling can be used today as any other tool of materials research, the same way all other physical and chemical methods are used (IR, Raman, NMR, Brillouin spectroscopies, X-ray and neutron diffraction, mass spectrometry, etc.)

Atomistic Modeling: Computational Tools

$N \sim$ 1,000-1000,000 atoms
$t \sim$ 1-10 ns
$\tau \sim 10^6$-10^7 time steps
$n \sim 10^6$-10^7 configurations

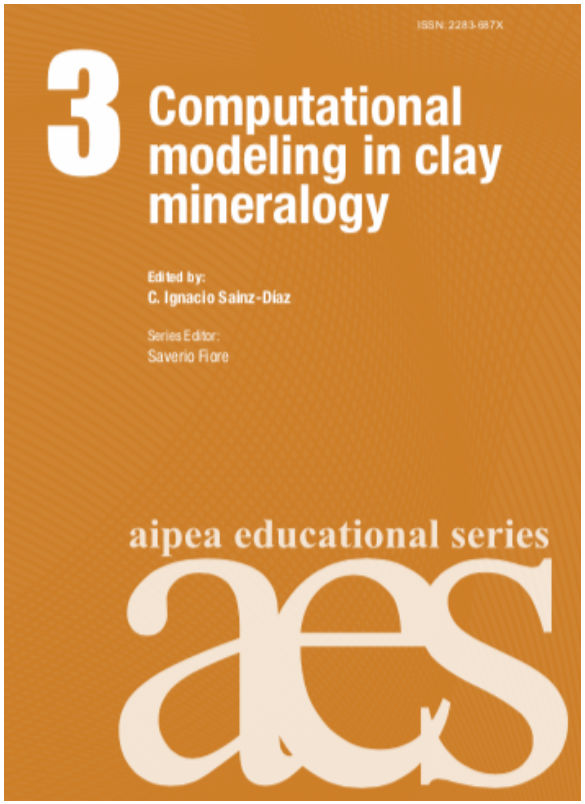

Atomistic computer modeling can be used today as any other tool of materials research, the same way all other physical and chemical methods are used (IR, Raman, NMR, Brillouin spectroscopies, X-ray and neutron diffraction, mass spectrometry, etc.)

Molecular Dynamics: Details of the Technique

Numerically solve Newtonian equation of motion for *N* interacting particles:

$\mathbf{r}_i(t+\Delta t) = \mathbf{r}_i(t) + \mathbf{v}_i(t)\Delta t + ½\,\mathbf{a}_i(t)\Delta t^2$; $\Delta t \sim 1$ fs $= 10^{-15}$ s

$\mathbf{a}_i = \mathbf{F}_i/m = [\, -\partial U(\mathbf{r}_1, \mathbf{r}_2, \ldots \mathbf{r}_N)/\partial \mathbf{r}_i \,]/m$; $i=1,2,\ldots,N$ ($N \sim 10^3 - 10^6$ atoms)

$$U = \Sigma\Sigma U_{ij} = \Sigma\Sigma(A_{ij}/r_{ij}^{12} - B_{ij}/r_{ij}^{6} + q_i q_j/\varepsilon_0 r_{ij}) + \Sigma\, ½k_b\,(r_{ij} - r_0)^2 + \Sigma\, ½k_\theta\,(\theta_{ij} - \theta_0)^2$$

Short-range repulsion | v-d-Waals | Coulombic | bond stretching | bond bending

Time averaging over a dynamic trajectory of the simulated system

Periodic boundary conditions (PBC)

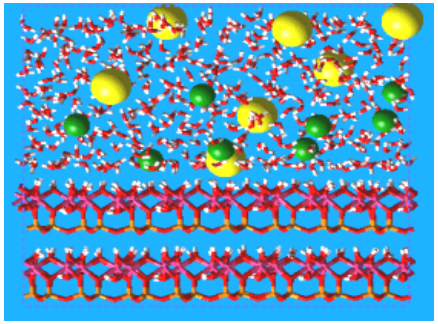

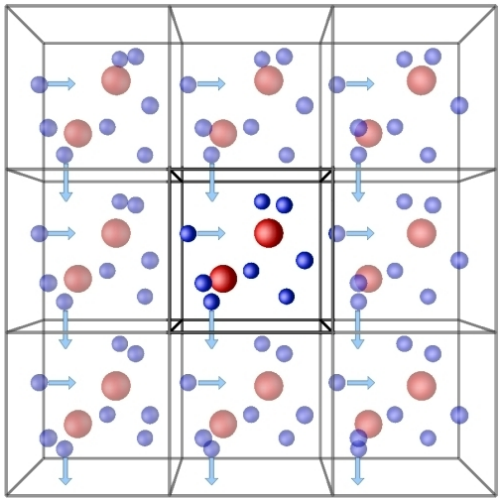

http://isaacs.sourceforge.net/phys/pbc.html

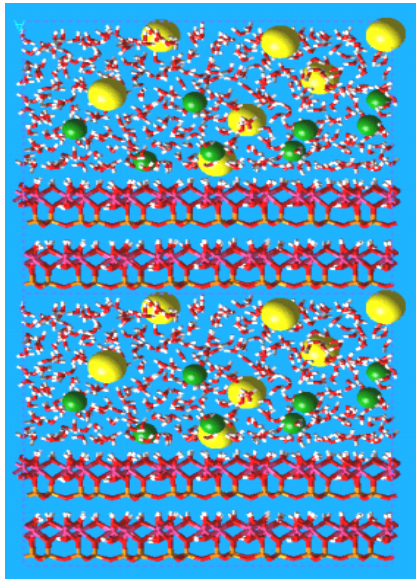

- ***CLAYFF*** – specialized semi-empirical fully flexible force field model allowing for realistic exchange of momentum and energy among all atoms – solid substrate and aqueous solution (Cygan, Liang, Kalinichev, *J.Phys.Chem. B*, **108** 1255-1266, 2004)

ClayFF Construction and Parametrization

1. **No explicit bonds – quasi-ionic**
2. **LJ parameters for all oxygen atoms are assumed to be equal to Ow for SPC water**

Both assumptions are great simplifications of reality, but they seem to work quite well

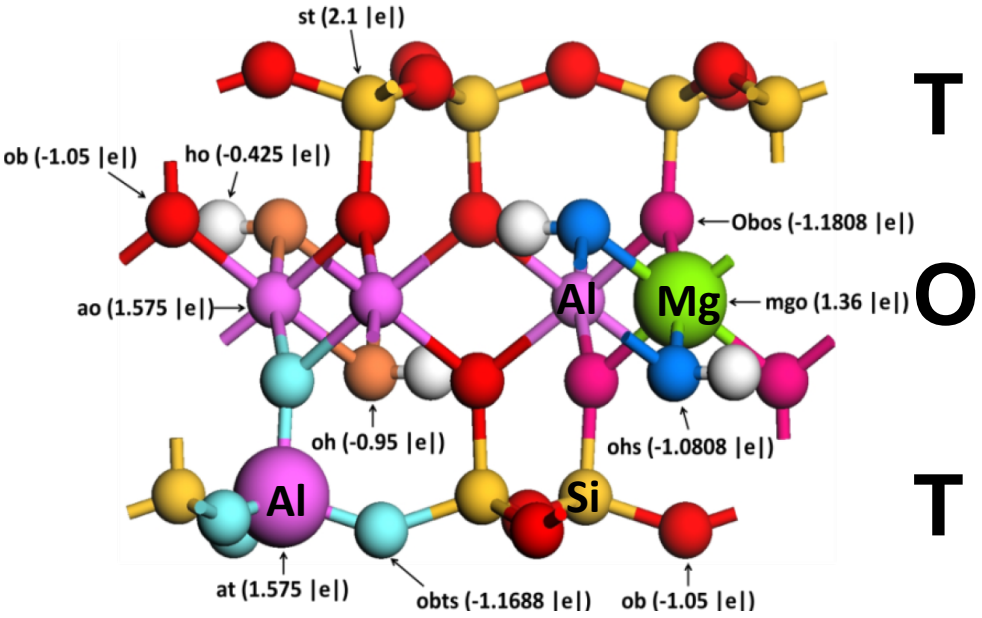

- Accurate determinations of partial charges are required to represent charge distributions of interlayer and external surfaces where electrostatic forces control sorption and transport processes
- Atomic charges derived from DFT calculations for cluster and periodic models of ***simple oxide and hydroxide phases*** (brucite, gibbsite, kaolinite, quartz…)
- Allows for ***charge delocalization*** among coordinating oxygens for substitutions

ClayFF: Cygan, Liang, Kalinichev, *J.Phys.Chem. B*, **108** 1255-1266 (2004)

Structure and Composition of Complex Clays

$Si_4Al_2O_{10}(OH)_2$
No substitutions
Non-swelling

Pyrophyllite

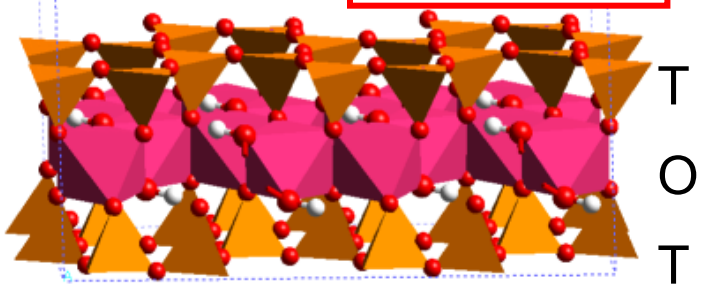

Illite (muscovite)

$K\ (Si_3Al)Al_2O_{10}(OH)_2$
Many substitutions
Many interlayer ions
1.0*e* charge per $O_{10}(OH)_2$
Non-swelling

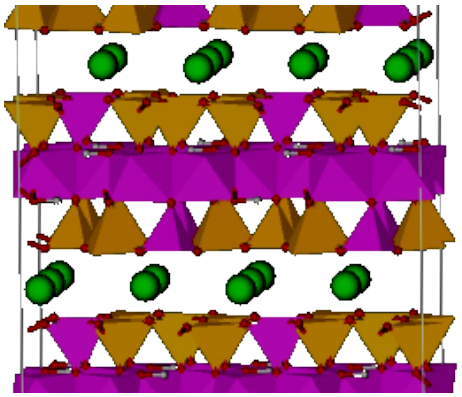

Dioctahedral Smectites

Smectite (montmorillonite)

$Na_3(Si_{31}Al)(Al_{14}Mg_2)O_{80}(OH)_{16}\cdot nH_2O$
Some tetrahedral Al sub
Mostly octahedral Mg sub
Swelling

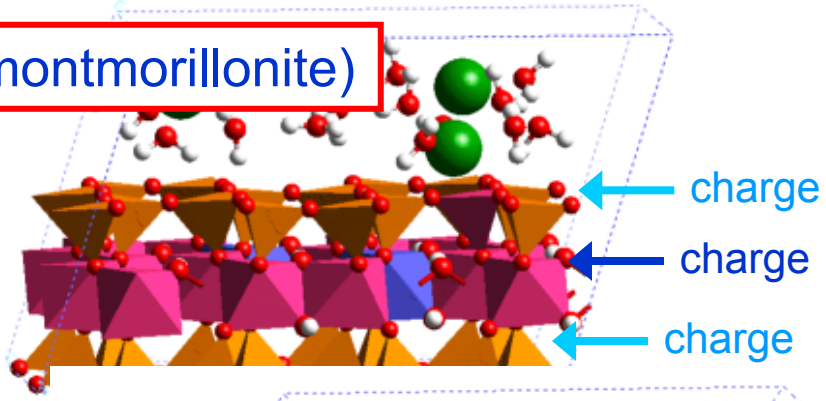

0.375*e* charge per $O_{10}(OH)_2$

Beidellite

$Na_3(Si_{29}Al_3)Al_{16}O_{80}(OH)_{16}\cdot nH_2O$
Mostly tetrahedral Al sub
Swelling

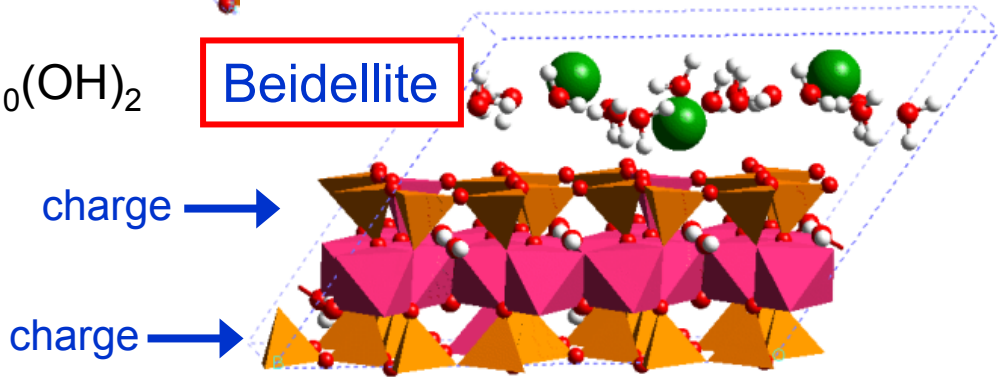

MD Modeling of Smectite-Solution Interfaces

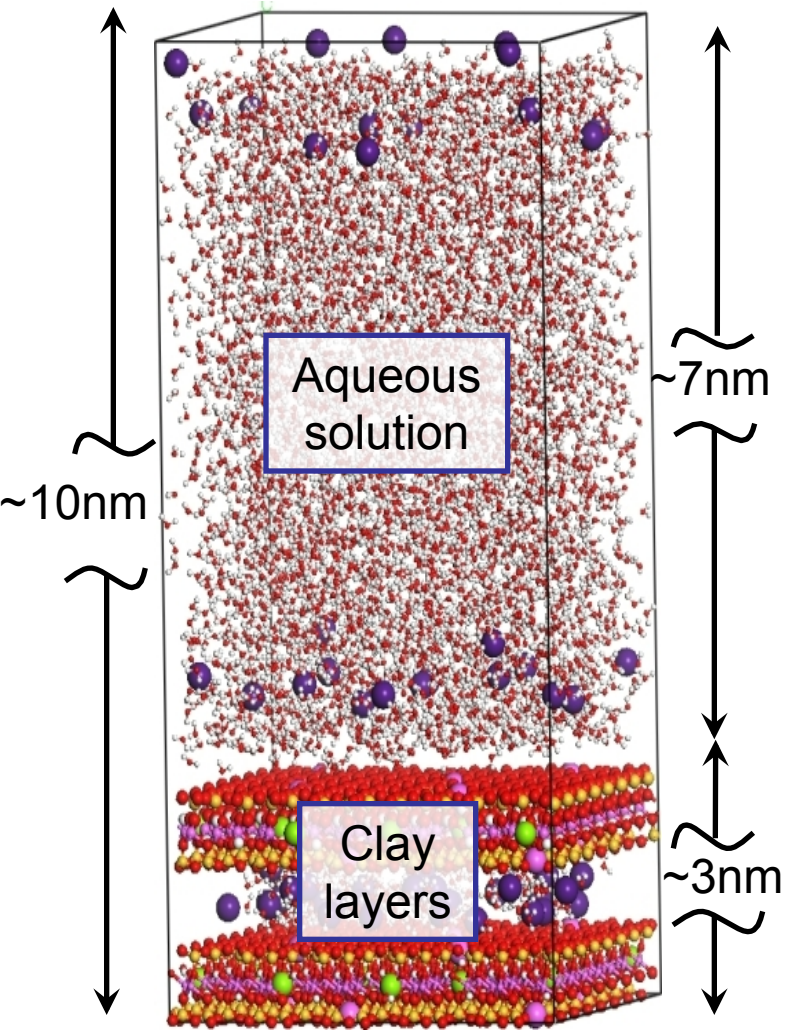

Classical Newtonian dynamics

- N_{tot} ~ 3,000 – 10,000 atoms
- N_{H2O} ~ 0 – 1,000 molecules
- *ClayFF* force field (Cygan et al., 2004)
- $a \times b \times c$ ~ $3 \times 3 \times 10$ nm^3
- Periodic boundary conditions
- *NVT*- or *NPT*-ensemble T=300K; P =1 bar
- t ~ 200 - 1,000 ps
- Δt = 0.5-1.0 fs

Solution structure:

- ✓ Atomic density profiles ($\perp$)
- ✓ Atomic density surface distributions ($\parallel$)
- ✓ Topology of the interfacial H-bond network

Dynamics:

- ✓ Diffusion coefficients (longer time scale)
- ✓ Spectra of vibrational and rotational dynamics (shorter time scale)

Association of Metal Cations with Clay Surfaces

Two-Layer Clay Hydrates

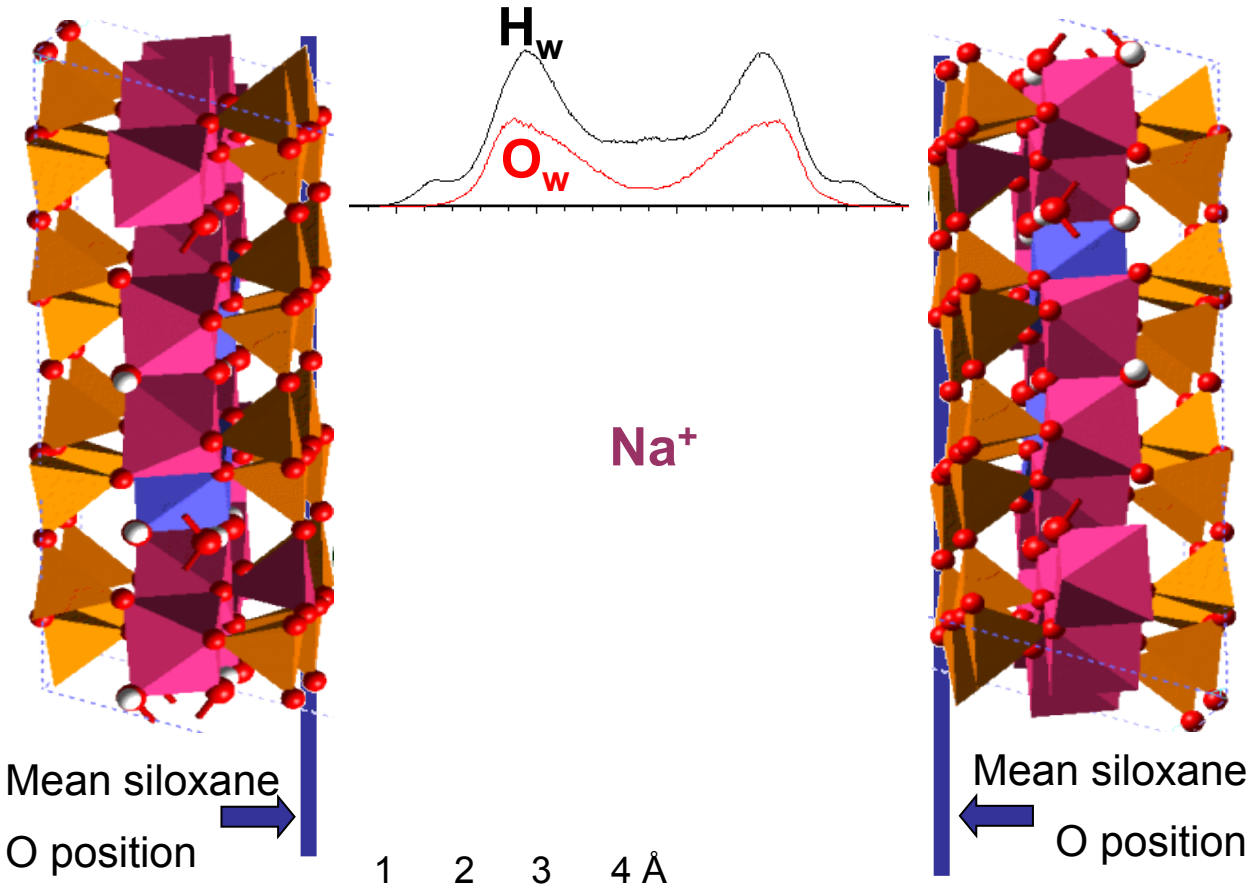

Pyrophyllite

Zero

Montmorillonite

Oct

Wyoming Montmorillonite

~Oct

Beidellite

Tet

Location of substitution sites in the clay structure can strongly influence the distribution and mobility of adsorbed ions and H_2O molecules

Swelling of Smectite (Montmorillonite)

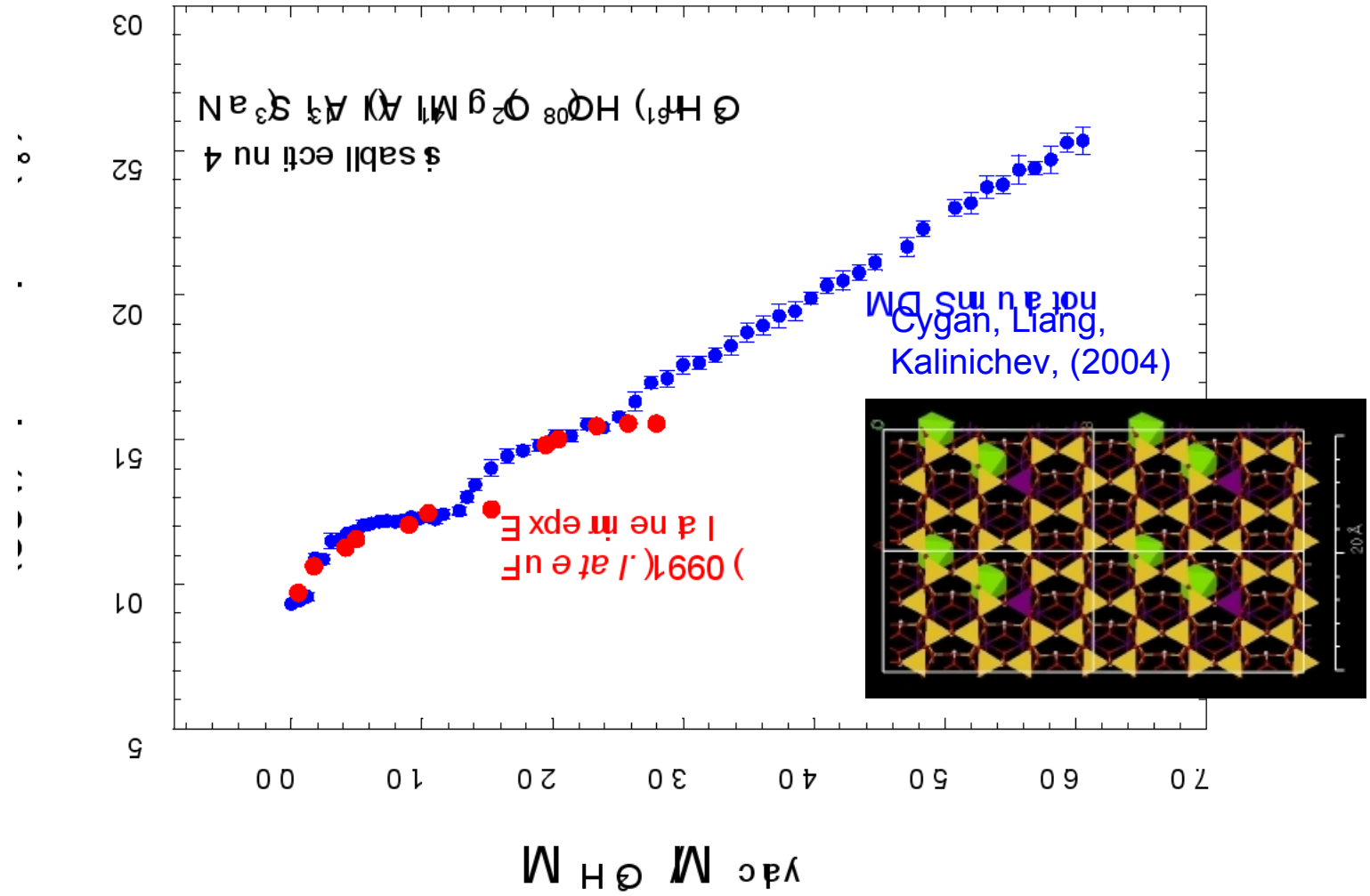

Water and Ions in Smectite Nanopores

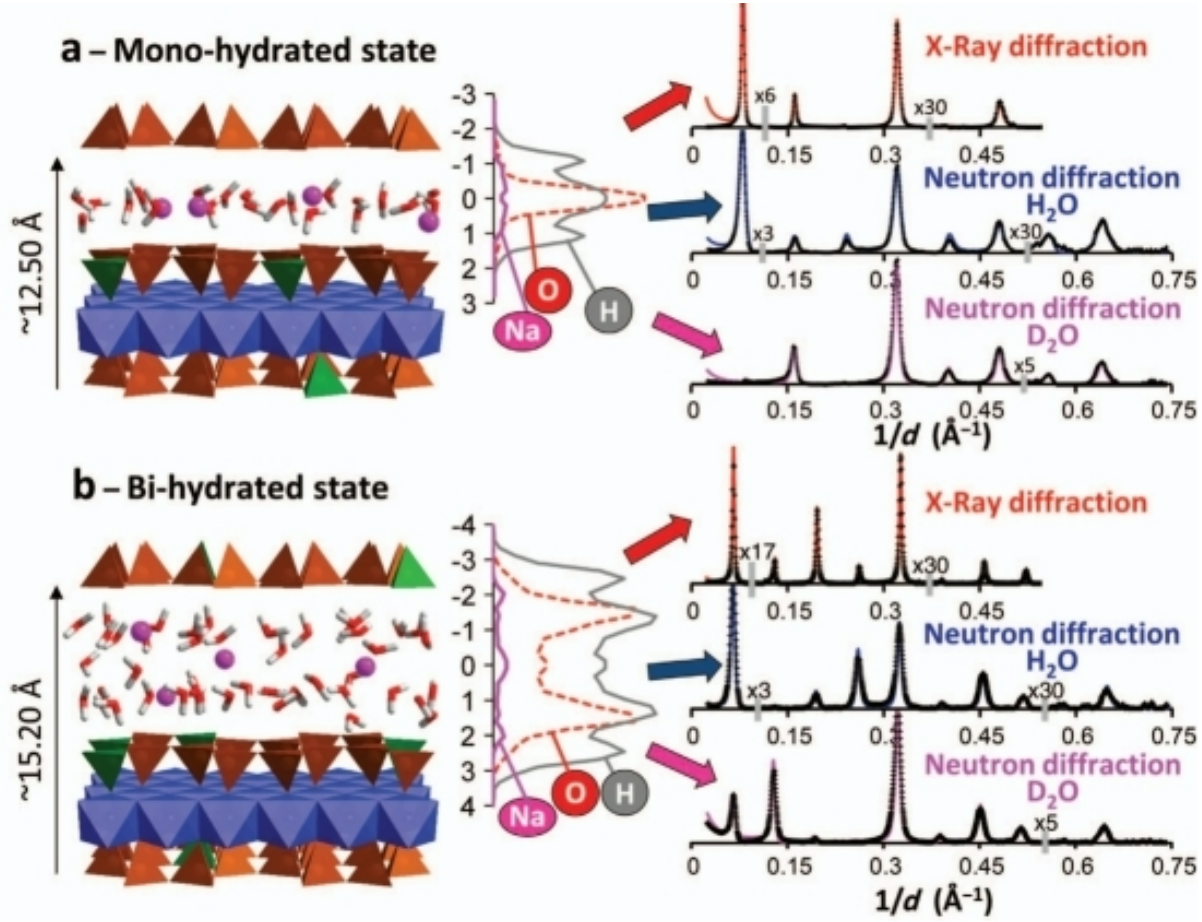

- ClayFF model better accounts for H_2O content and organization compared to earlier models.
- However, diffraction patterns for bi-hydrated samples from ClayFF simulations do not satisfactorily match the experimental data.
- Modification of ClayFF Lennard-Jones parameters was suggested that allows matching experimental water contents and fitting the complete set of diffraction data.
- Relevant information may thus be derived on the influence of layer charge on the orientational properties of interlayer water molecules for different clay models.

Ferrage et al., *J.Phys.Chem.C*, 2011, **115**, 1867-1881

Ferrage et al., *Clays and Clay Minerals*, 2016, **64**, 348-373

Structure and Diffusion at Smectite–Water Interfaces

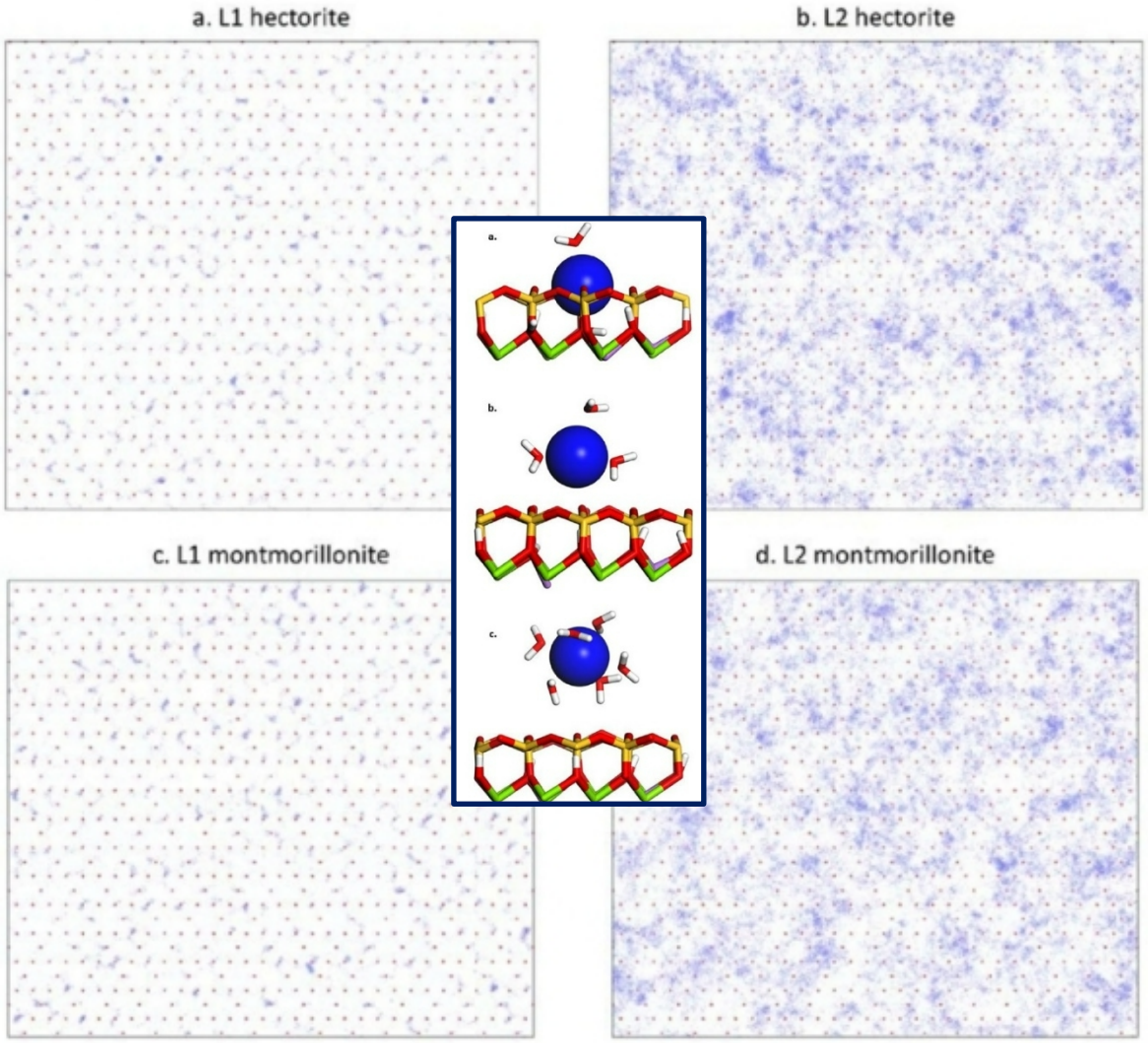

- There are only subtle differences in Na^+ adsorption complexes and water structure in the first adsorbed layer due to different arrangements of layer hydroxyl groups in the two clay models.
- The extent of surface disruption on bulk-like solution structure and diffusion extends to only a few water layers.
- A comparison of Na^+ residence times confirms similar behavior of inner-sphere and outer-sphere surface complexes at each clay surface, but ~1% of Na^+ ions adsorb in ditrigonal cavities on the hectorite surface.
- The presence of these anhydrous ions is consistent with highly immobile anhydrous ions seen in previous nuclear magnetic resonance spectroscopic measurements of hectorite pastes.

Greathouse et al., *J.Phys.Chem.C*, 2015, **119**, 17126-17136

H_2O Orientation at the Smectite-Water Interface

MD simulations show **two principal orientations of H_2O molecules** close to the clay surface : **monodentate** and **bidentate**:

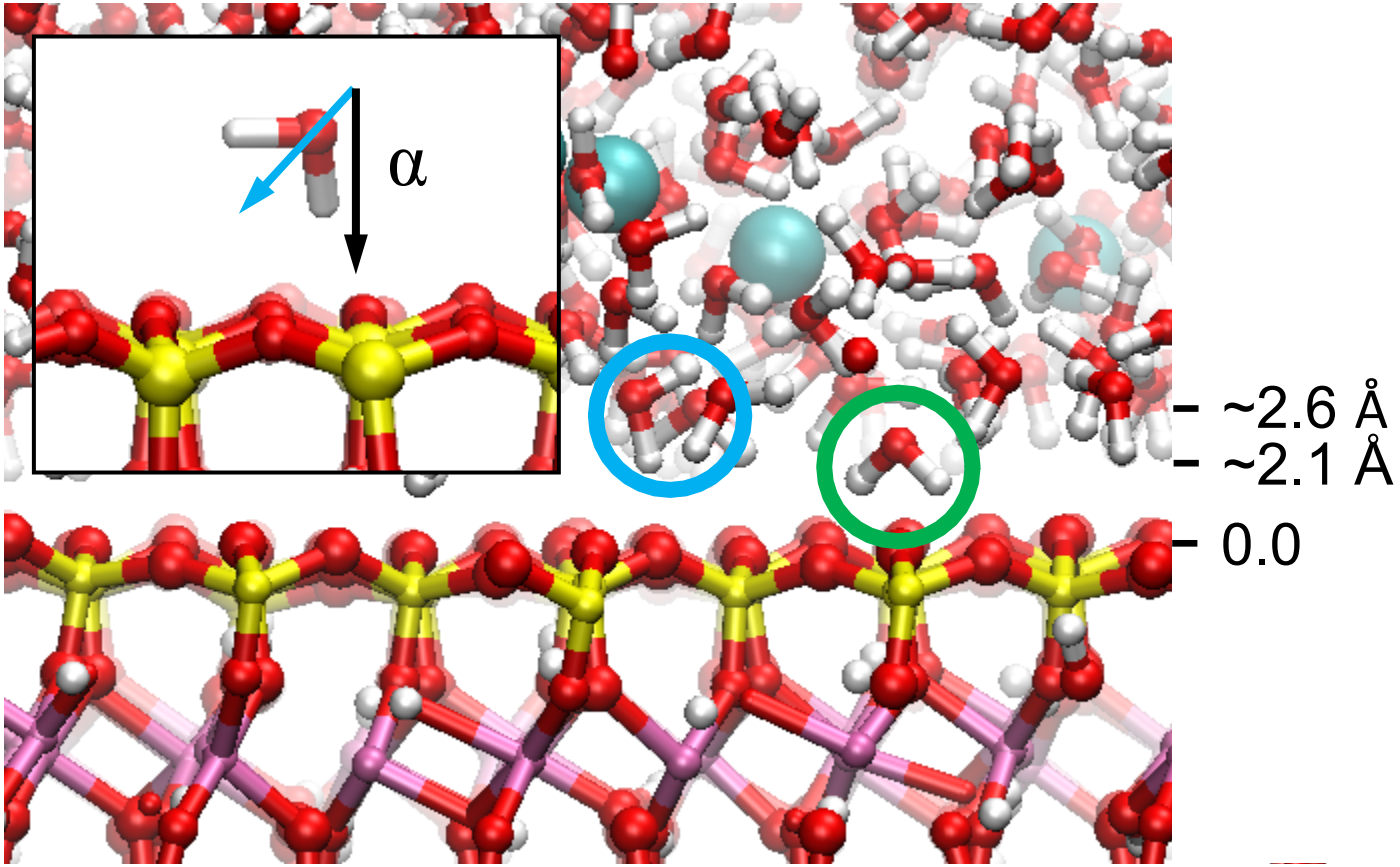

Hydrogen Bonding of H_2O at the Smectite Surface – Nature of the Sharp OH Vibrational Band

Kuligiewicz et al., *Clays and Clay Minerals,* **63**, 15-29 (2015)

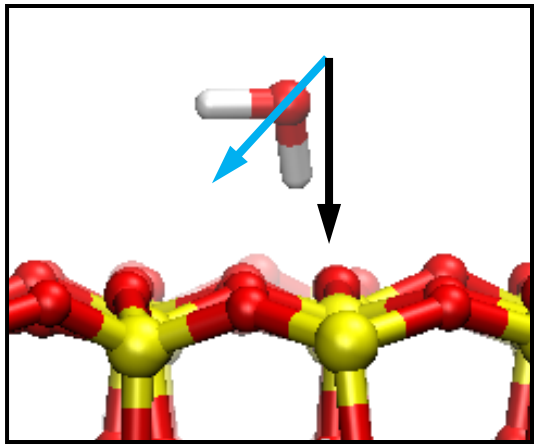

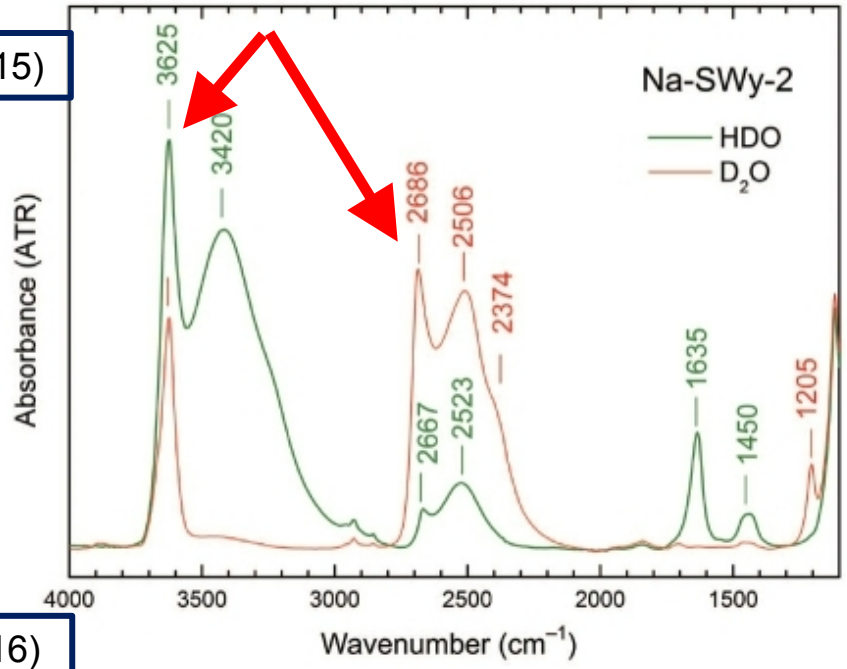

Szczerba et al., *Clays and Clay Minerals,* **64**, 452-471 (2016)

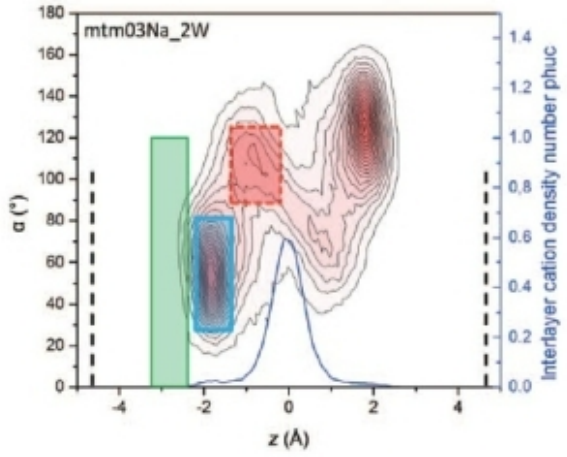

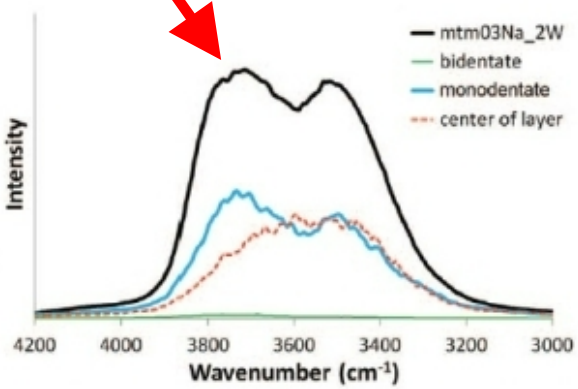

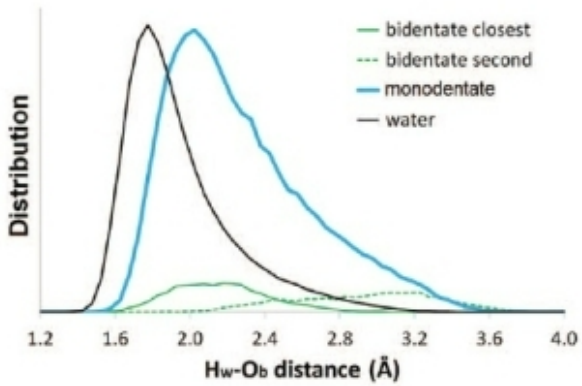

Hydrophobicity of Smectite Clay Surfaces (I)

M.Szczerba, M.Kowalik, A.G.Kalinichev, *Appl.Clay Sci.*, **188,** 105497 (2020)

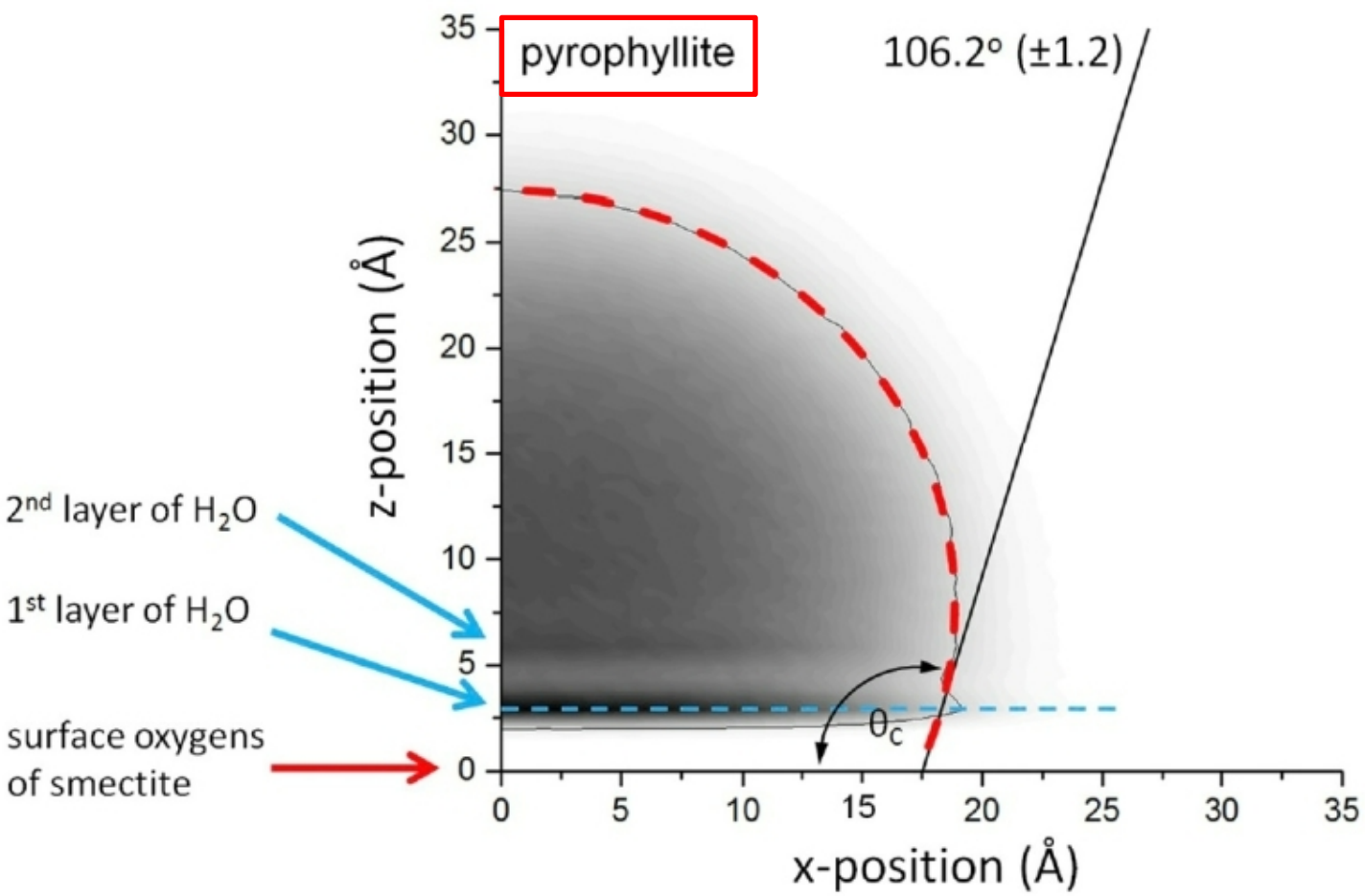

Hydrophobicity of Smectite Clay Surfaces (II)

M.Szczerba, M.Kowalik, A.G.Kalinichev, *Appl.Clay Sci.*, **188,** 105497 (2020)

Montmorillonite

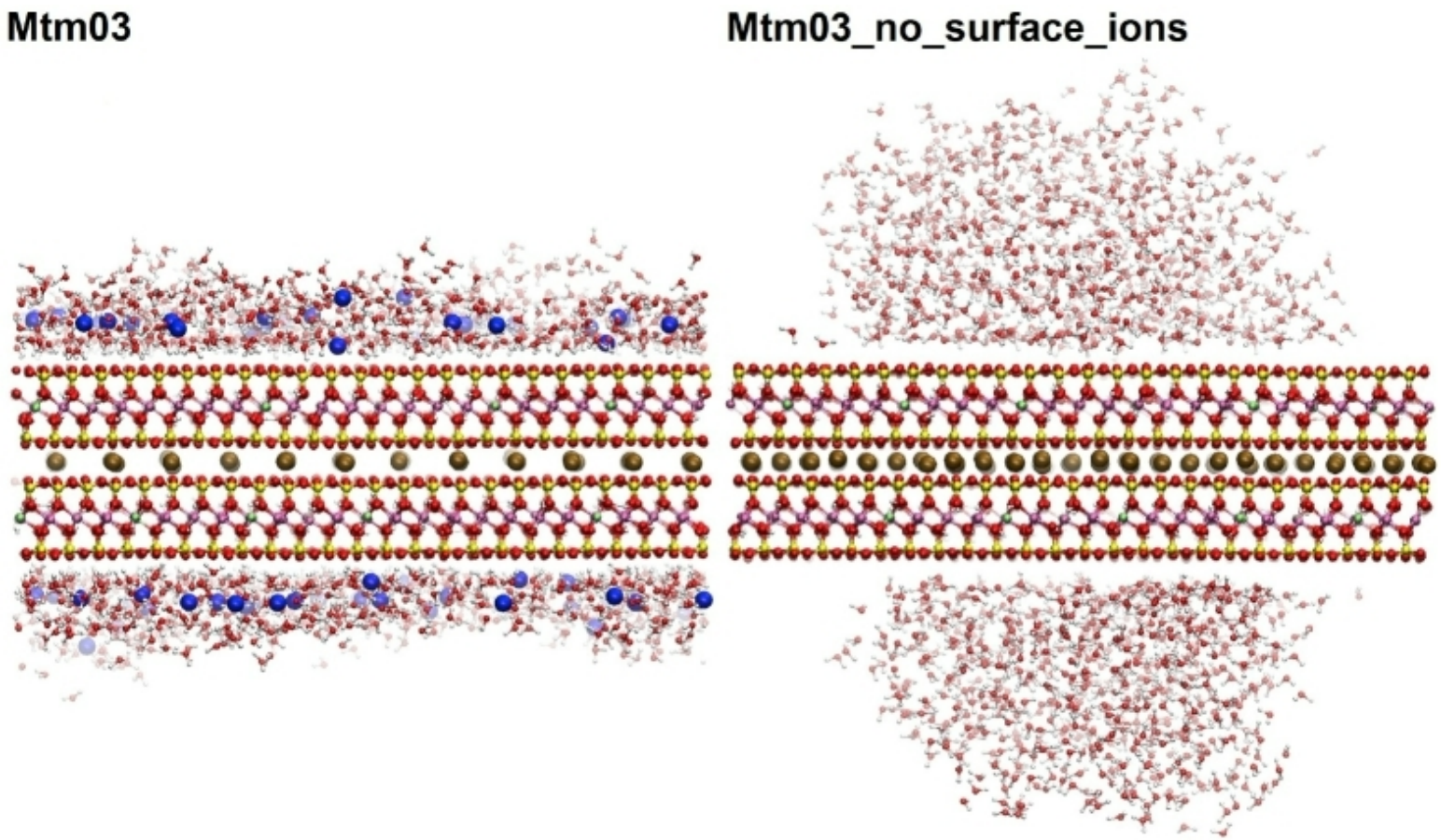

Hydrophobicity of Smectite Clay Surfaces (III)

M.Szczerba, M.Kowalik, A.G.Kalinichev, *Appl.Clay Sci.*, **188,** 105497 (2020)

Montmorillonite

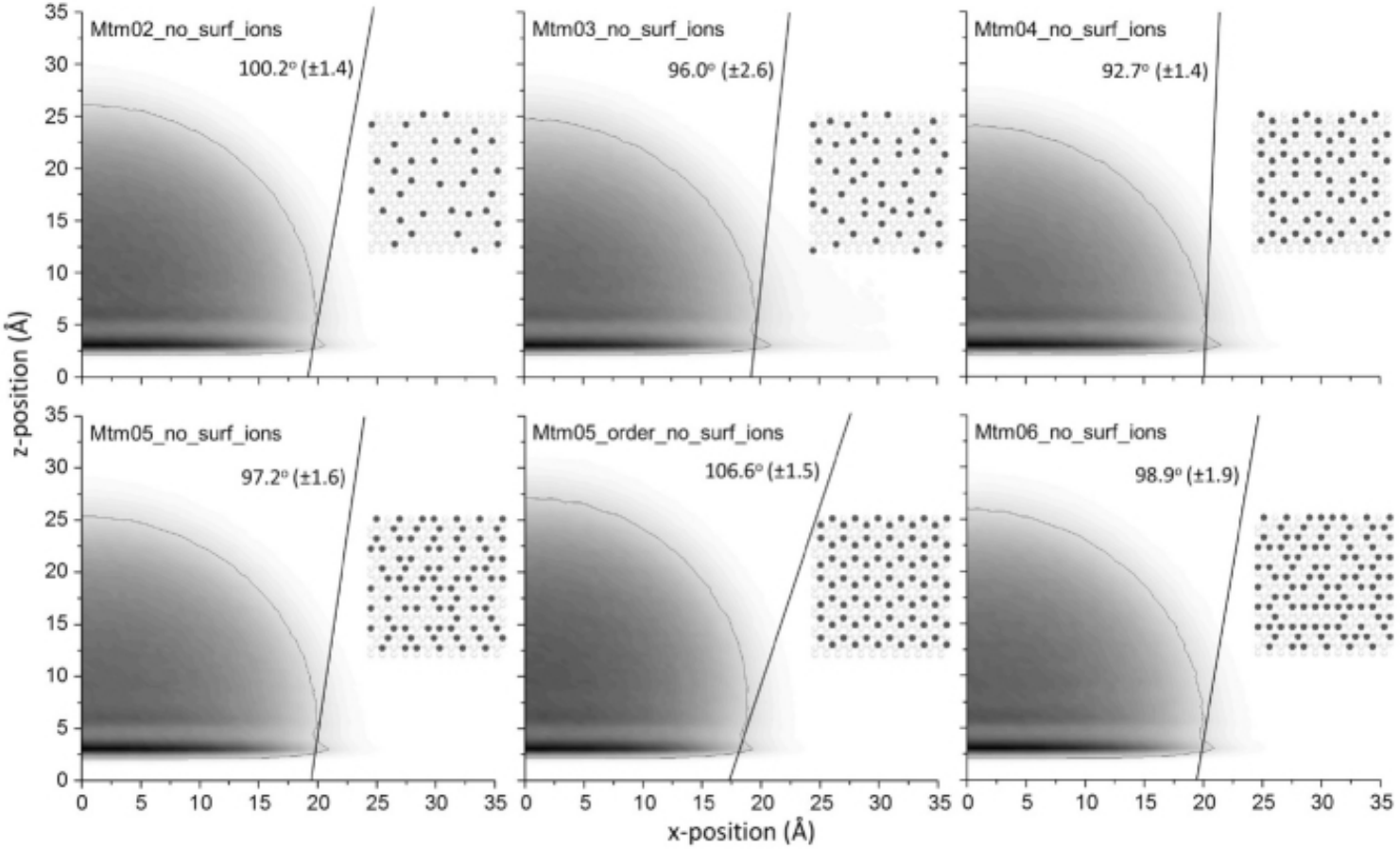

Orientation of H_2O Molecules on Montmorillonites

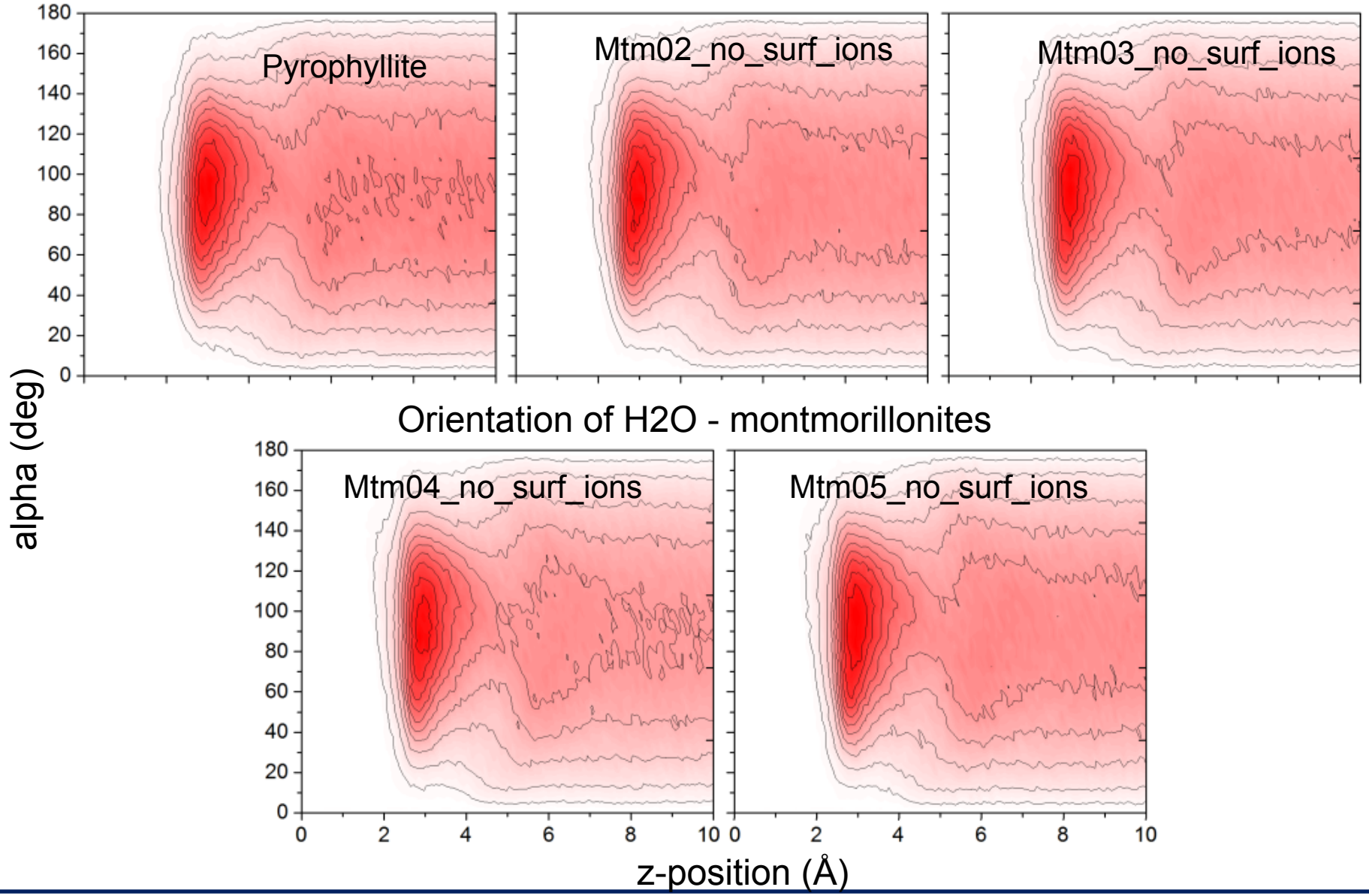

Orientation of H2O - montmorillonites

Hydrophobicity of Smectite Clay Surfaces (IV)

M.Szczerba, M.Kowalik, A.G.Kalinichev, *Appl.Clay Sci.*, **188,** 105497 (2020)

Beidellite

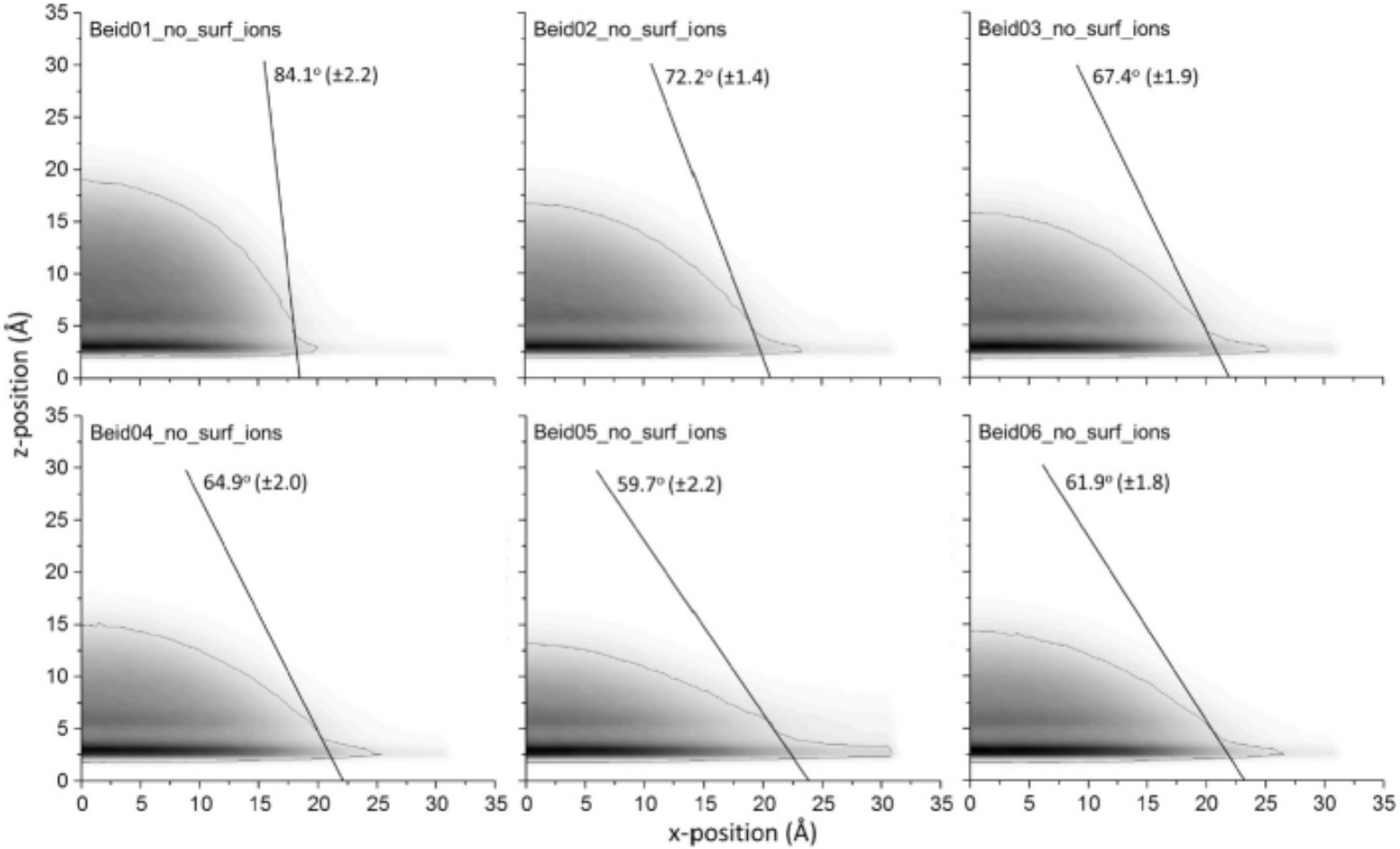

Orientation of H_2O Molecules on Montmorillonites

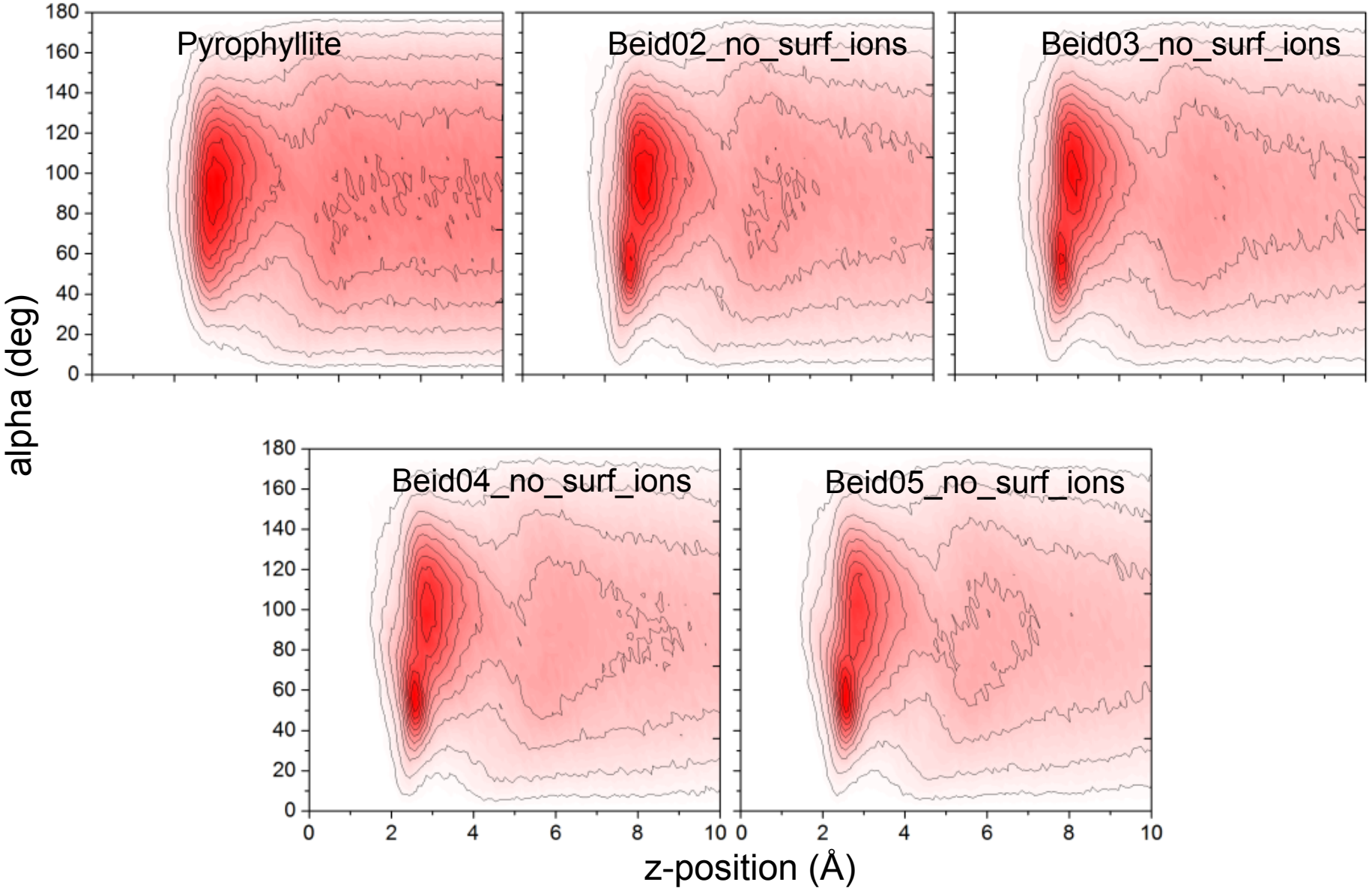

Hydrophilicity / Hydrophobicity of Smectite Surface

- **The hydrophobicity of the smectite surfaces** depends on our **definition of the surface**:
  - if charge-balancing cations are considered part of the surface, it is highly hydrophilic;
  - however, the surface itself, with the counter-ions removed, is quite hydrophobic
- **The orientation of H_2O molecules** on smectite surfaces is significantly different for the surface with ions and the same surface from which all the ions are removed
  - the surface itself is intrinsically hydrophobic
  - the hydrophilicity is primarily due to the charge-balancing cations on the surface
- **Hydrophobic** smectite surfaces are favorable for the adsorption of **organic molecules**

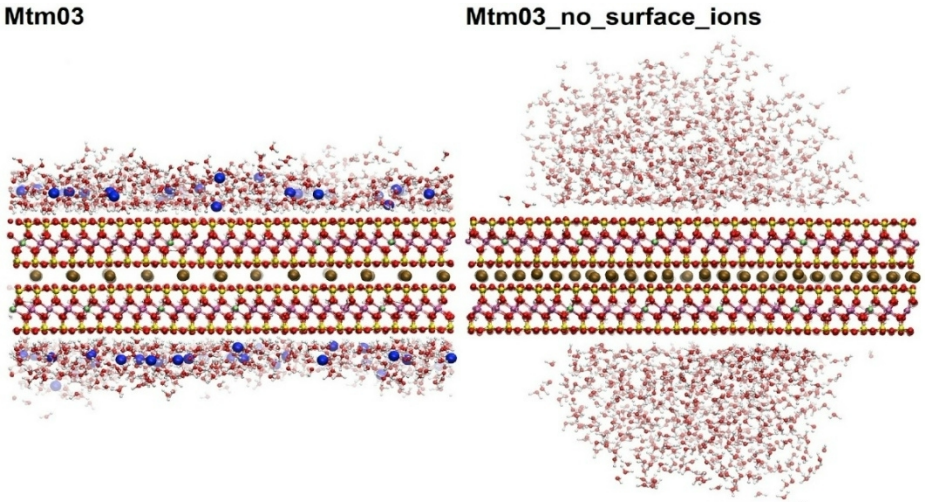

Effects of the Charge Localization on the Adsorption and Transport of Ions in $3M^{+}(Si_{31}Al)(Al_{14}Mg_2)O_{80}(OH)_{16}\cdot nH_2O$ (M^{+} = Li^{+}, Na^{+}, K^{+}, Rb^{+}, Cs^{+}, $½Ca^{2+}$, $½Sr^{2+}$, $½Ba^{2+}$, $½Ni^{2+}$)

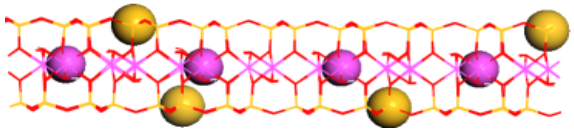

Pyrophillite atomic structure from X-ray

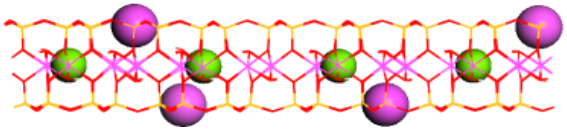

Uniform distribution in T and O layers (Uni)

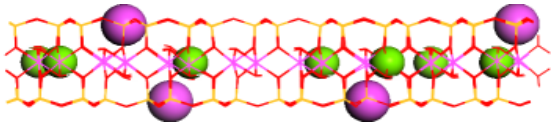

Random distribution in O layers (RanO)

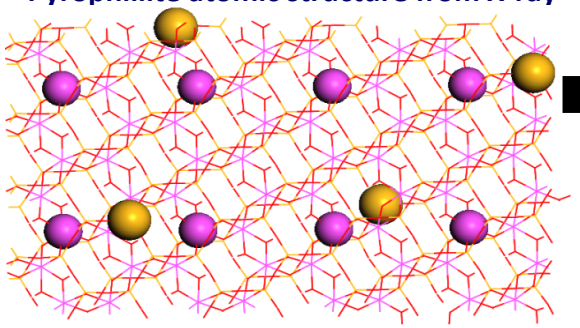

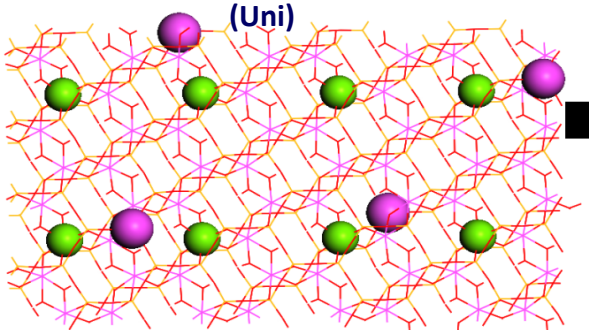

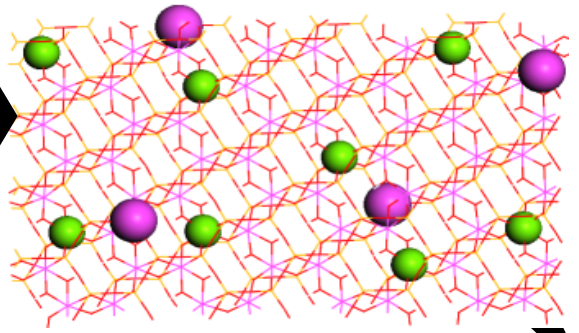

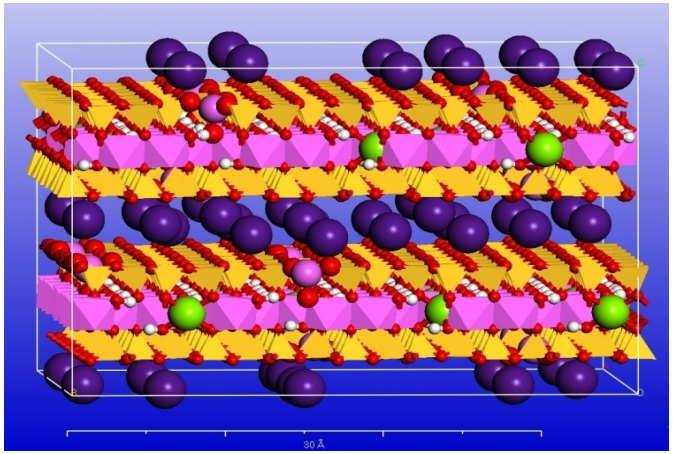

Oxygen

Silicon

Aluminum

Magnesium

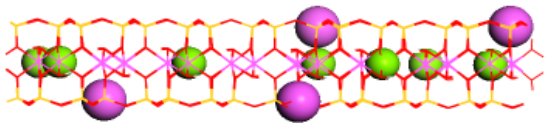

Random distribution in O and T layers (RanTO)

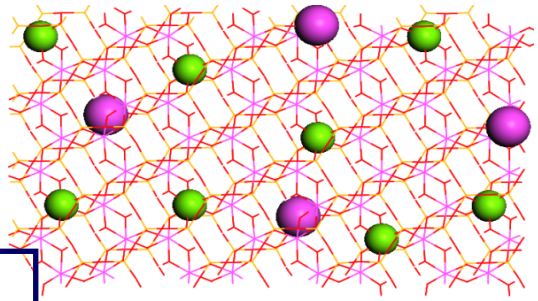

B.F.Ngouana Wakou, A.G.Kalinichev, *J.Phys.Chem.C,* **118**, 12758 (2014)

Interlayer and Surface Adsorption Sites on (001) of Cs^+ -Montmorillonite Smectite

B.F. Ngouana Wakou, A.G.Kalinichev
J. Phys. Chem. C, **118**, 12758-12773 (2014)

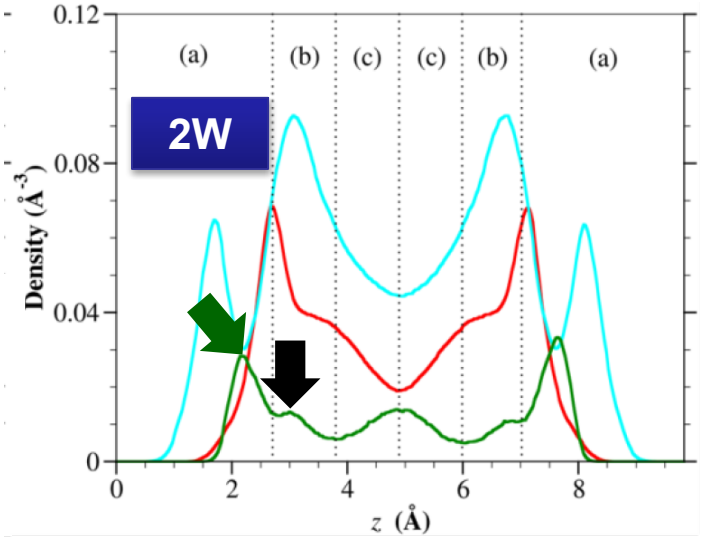

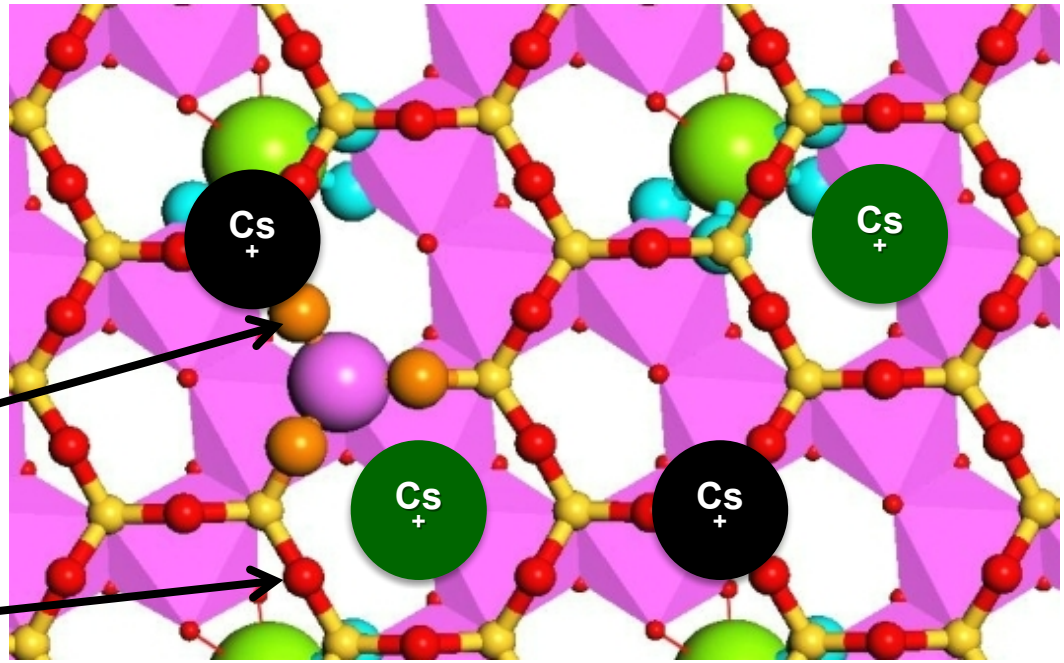

O_{bts} (-1.17 |e|)

O_b (-1.05 |e|)

Water Structure and Aqueous Uranyl(VI) Adsorption Equilibria onto External Surfaces of Beidellite, Montmorillonite, and Pyrophyllite

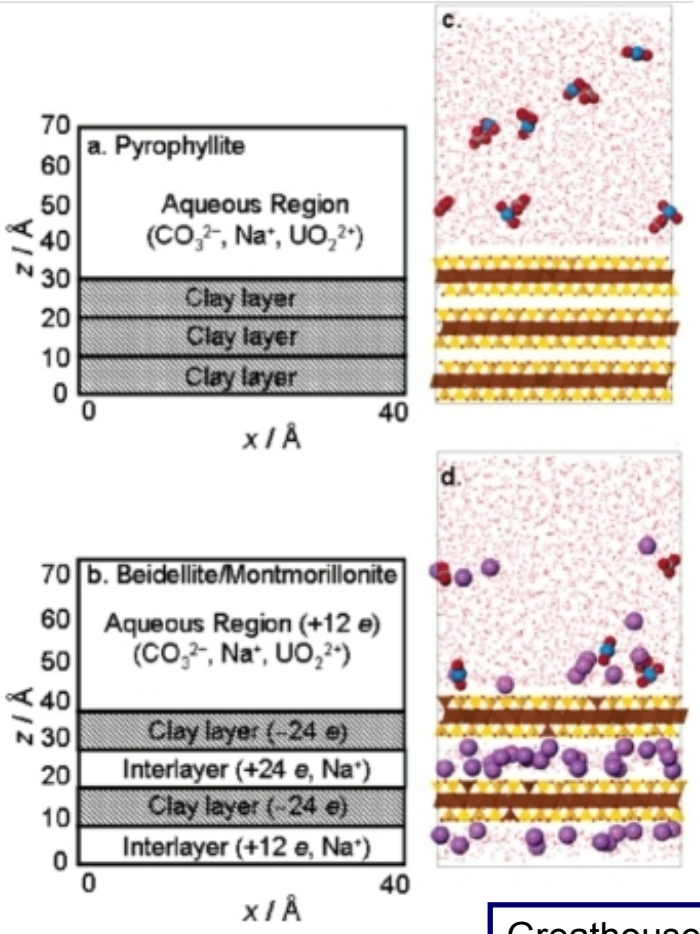

- Aqueous UO_2^{2+} concentration from 0.027 to 0.162 M.
- Na^+ ions and CO_3^{2-} ions (0.027-0.243 M) were present in solution to realistically model a stream of uranyl-containing groundwater contacting a mineral system comprised of Na-smectite.
- No adsorption occurred near the pyrophyllite surface.
- Little difference in UO_2^{2+} adsorption onto the beidellite and montmorillonite, despite the difference in location of clay layer charge.
- At low uranyl concentration, the penta-aquo-uranyl complex dominates in solution and readily adsorbs to the clay basal plane.
- At higher uranyl (and carbonate) concentrations, the mono(carbonato) complex forms in solution, and uranyl adsorption decreases.

Greathouse J.A., Cygan R.T, *Phys.Chem.–Chem.Phys.*, 2005, **7**, 3865-3871; *Env. Sci. Technol.*, 2006, **40**, 3580-3586

Free Energy of Ion Surface Adsorption

Potential of Mean Force:

$$W(z) = -k_B T \ln\left(\rho(z)\right) + const$$

z - distance from the surface

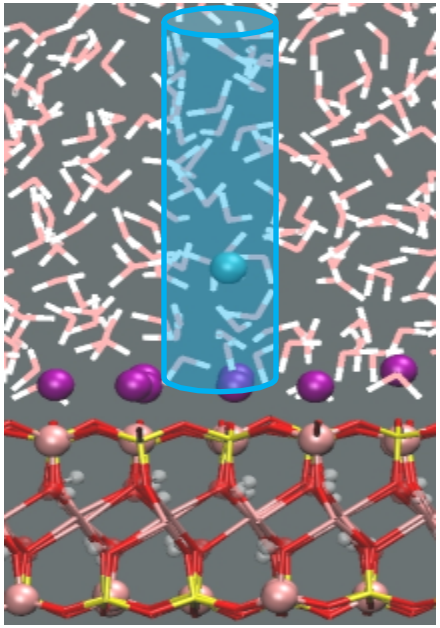

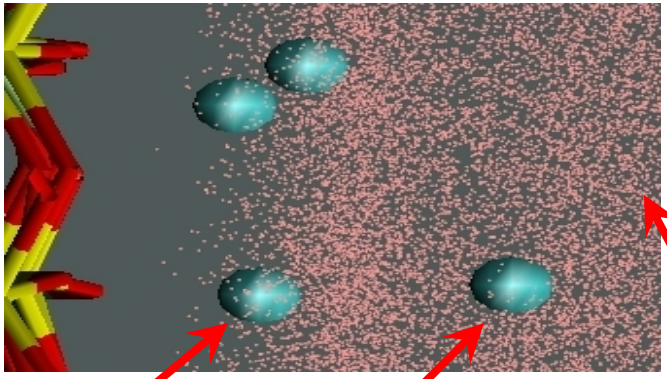

$$\mathbf{S{\cdot}I \Leftrightarrow S \cdot I(H_2O)_n \Leftrightarrow S + I}$$

ISSC OSSC desorbed ions

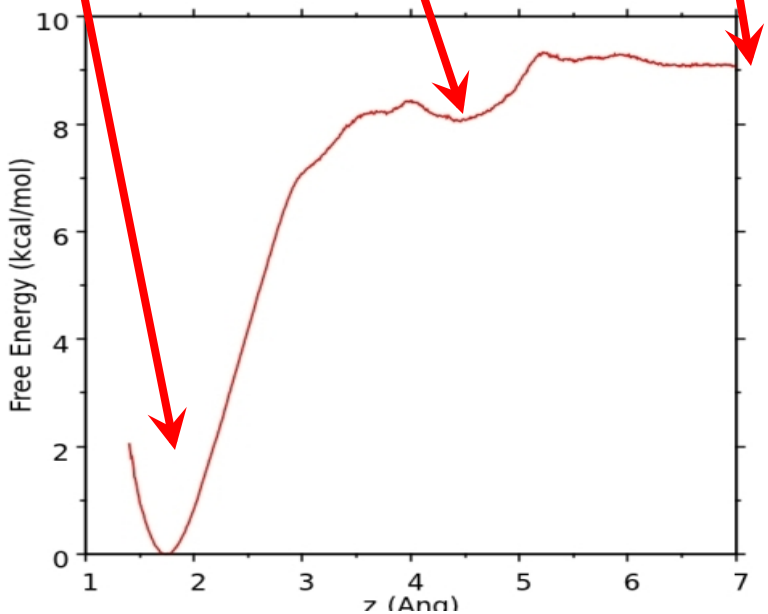

$$K_{eq} = \frac{4\pi \int \exp(-W_{ISSC}/k_B T)\, r^2 dr}{4\pi \int \exp(-W_{OSSC}/k_B T)\, r^2 dr}$$

Surface Sites and Adsorption Free Energy Profiles of UO_2^{2+} on Muscovite

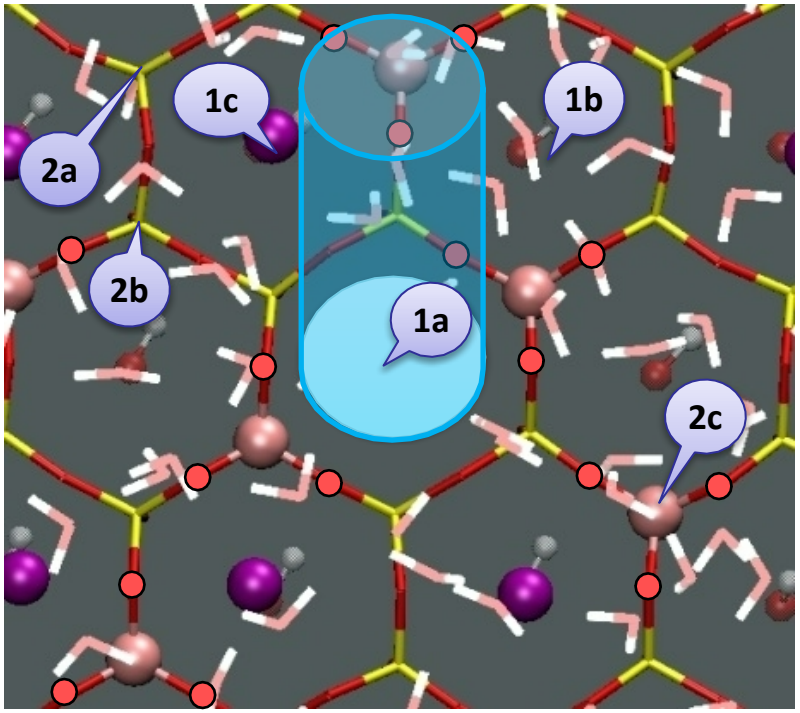

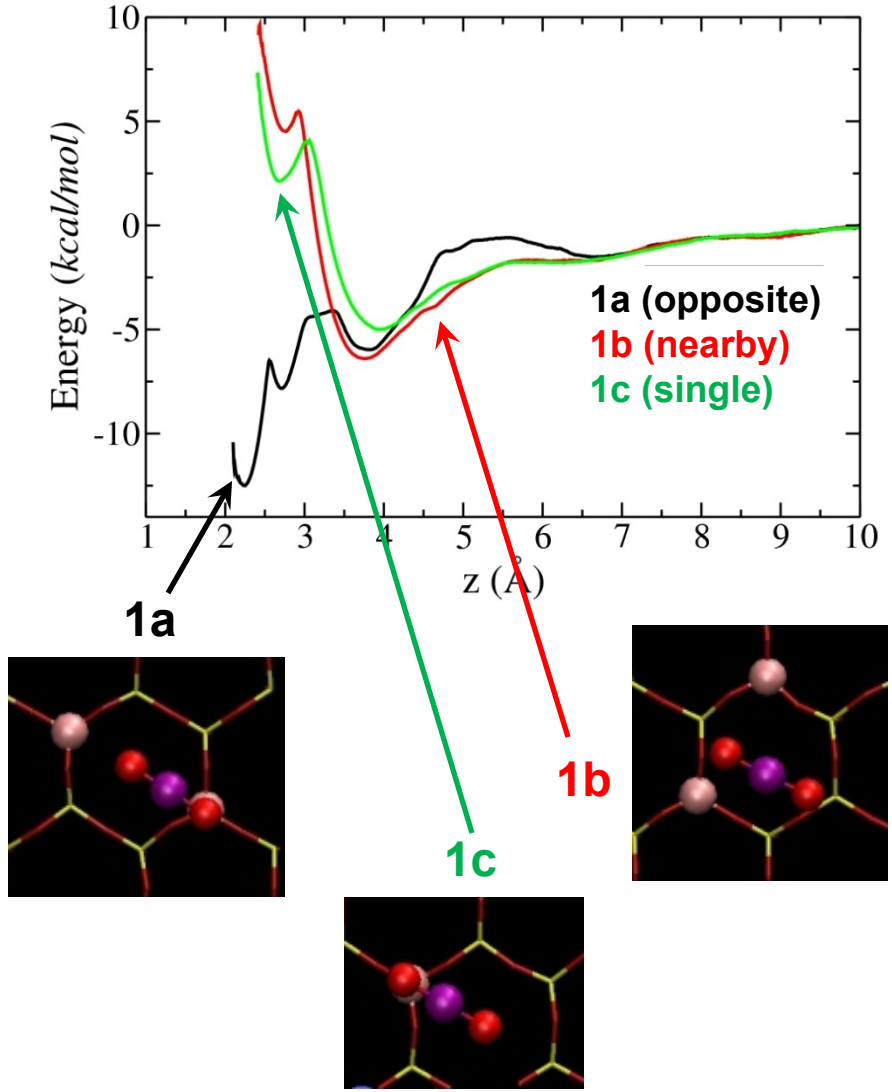

$$K_{eq} = \frac{4\pi \int \exp(-W_{ISSC}/k_B T)\, r^2 dr}{4\pi \int \exp(-W_{OSSC}/k_B T)\, r^2 dr}$$

N. Loganathan, A.G.Kalinichev, 2022, in prep.

Adsorption of Aqueous Crude Oil Components on the Basal Surfaces of Clay Minerals

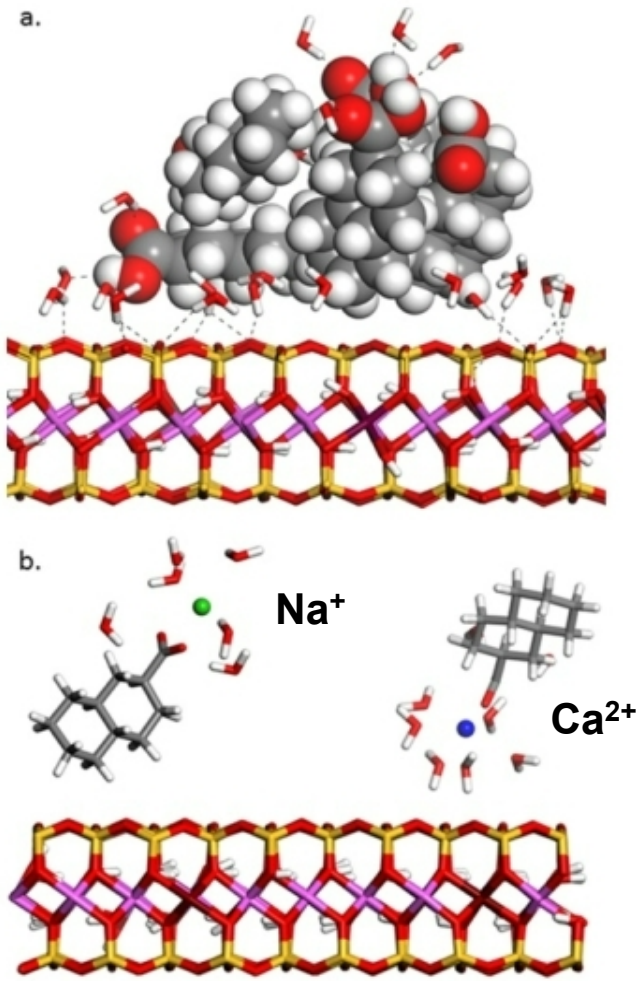

- Decahydro-2-naphthoic acid (DHNA and $DHNA^-$) as model crude oil components.
- The extent of adsorption is controlled by the hydrophilic nature and layer charge of the clay mineral.
- All organic species preferentially sorb on hydrophobic mineral surfaces.
- Analysis of cation−organic complexing in both the adsorbed and desorbed states reveals a strong preference for organic anions to coordinate with divalent Ca^{2+} ions rather than monovalent Na^+ ions, lending support to current theories regarding low-salinity water flooding.

Greathouse et al., *J.Phys.Chem.C*, 2017, **121**, 22772-22786

Mg-Salen Compounds as Subsurface Fluid Tracers: Molecular Dynamics Simulations in Toluene-Water Mixtures and Clay Mineral Nanopores

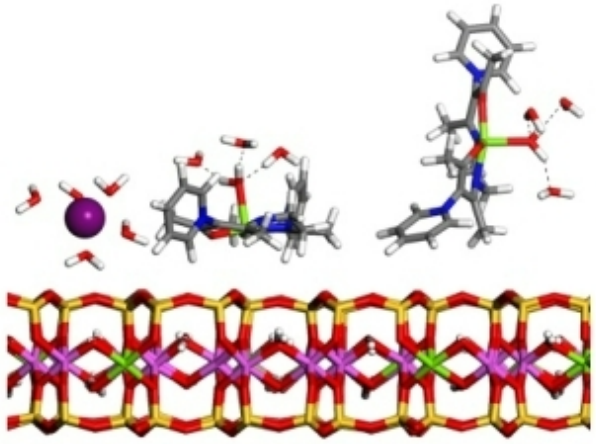

c. water-filled Na-montmorillonite nanopore

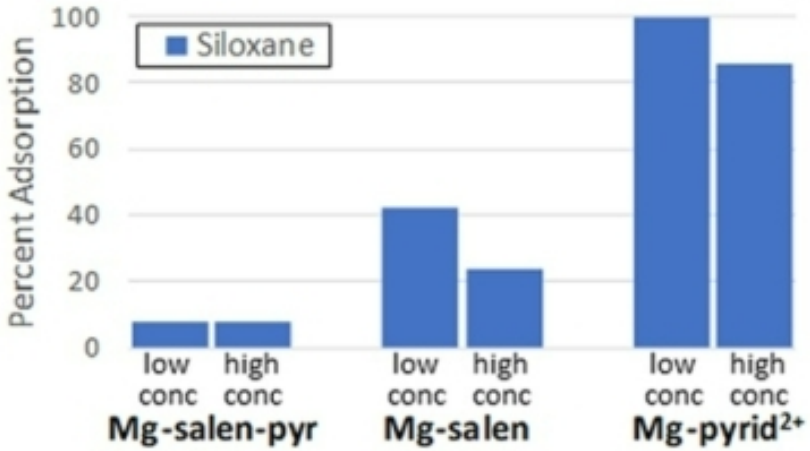

- Simulations of these complexes in fluid-filled mineral nanopores containing neutral (kaolinite) and negatively charged (montmorillonite) mineral surfaces reveal that adsorption tendencies depend upon a variety of parameters, including tracer chemical properties, mineral surface type, and solvent type (water or toluene).
- Simulation snapshots and averaged density profiles reveal insight into the solvation and adsorption mechanisms that control the partitioning of these complexes in mixed liquid phases and nanopore environments.
- The utility of molecular simulation in the design and screening of molecular tracers for use in subsurface applications is demonstrated

Greathouse et al., *Energy & Fuels* 2018, **32**, 4969-4978

Interaction of Natural Organic Matter with Clay Surfaces and NOM Aggregation in Clay Mesopores

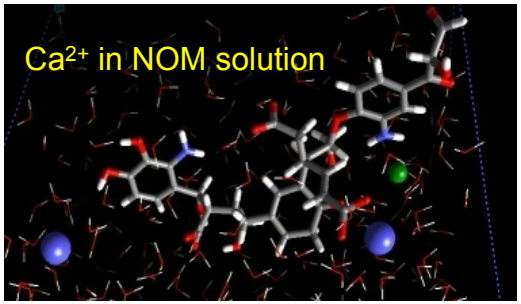

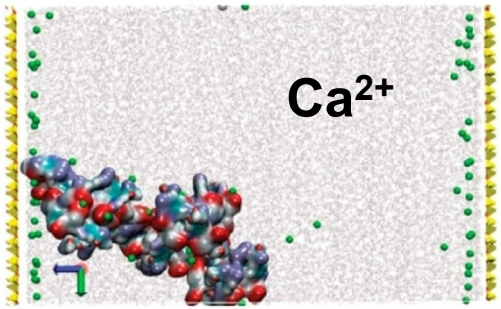

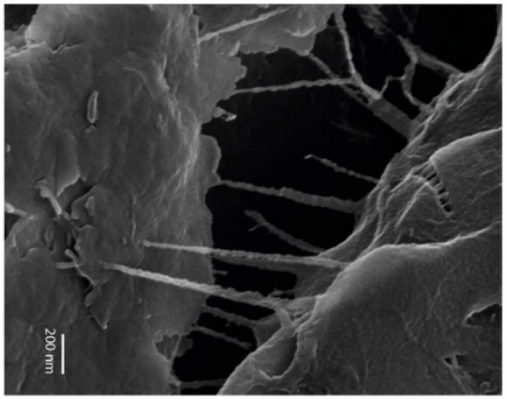

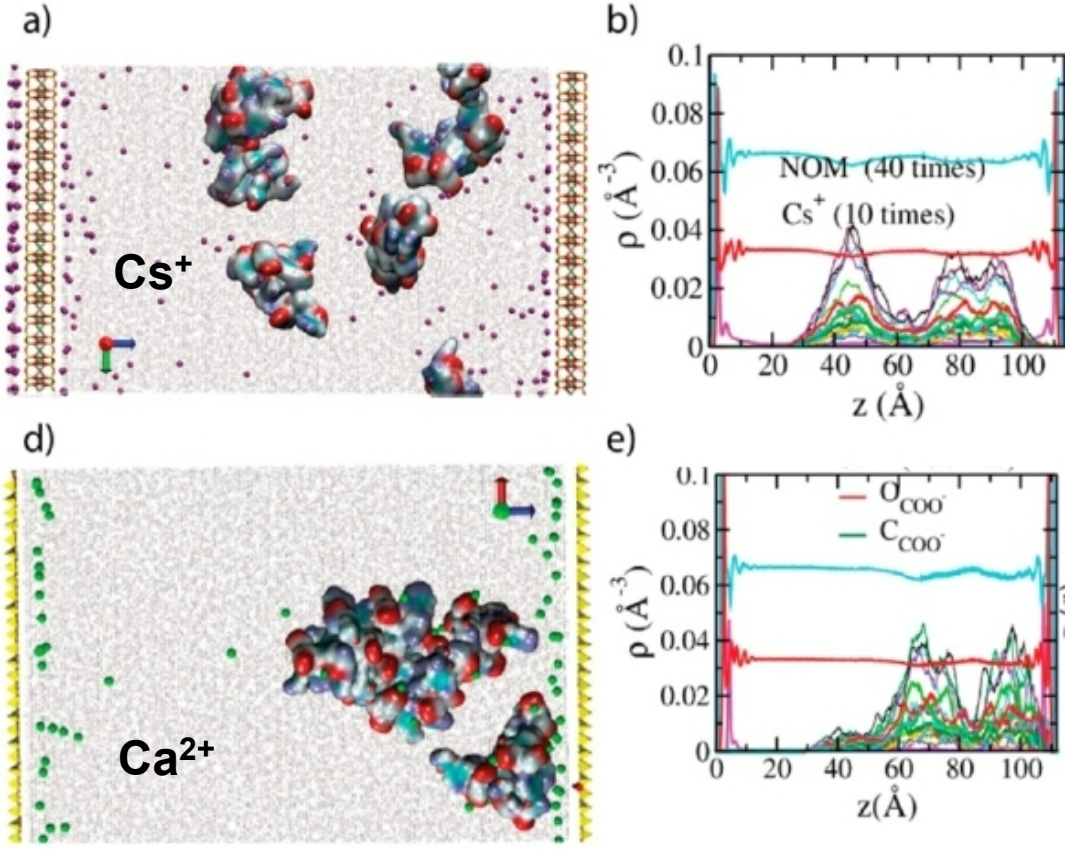

Greathouse et al., *Minerals*, 2012, **4**, 519-540

Loganathan et al., *J.Phys.Chem.A*, 2020, **124**, 9832-9843

MD Simulations of CO_2 Intercalation in Hydrated Na-Montmorillonite

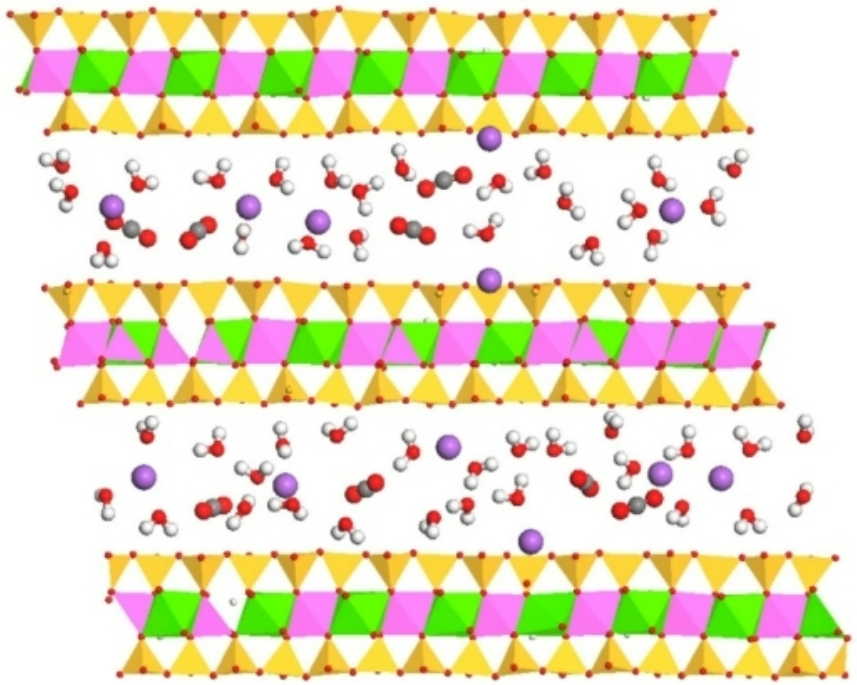

- The degree of swelling caused by intercalation of CO_2 strongly depends on the initial water content in the interlayer space.
- CO_2 intercalation stimulates inner-sphere adsorption of the positively charged interlayer ions on the internal clay surfaces, which modifies the wetting properties of the surfaces.

Cygan et al., *J.Phys.Chem.C*, 2012, **116**, 13079−13091

Myshakin et al., *J.Phys.Chem.C*, 2013, **117**, 11028−11039

Effect of Interlayer Cation Size and Charge on the Intercalation of CO_2 and H_2O into Hectorite

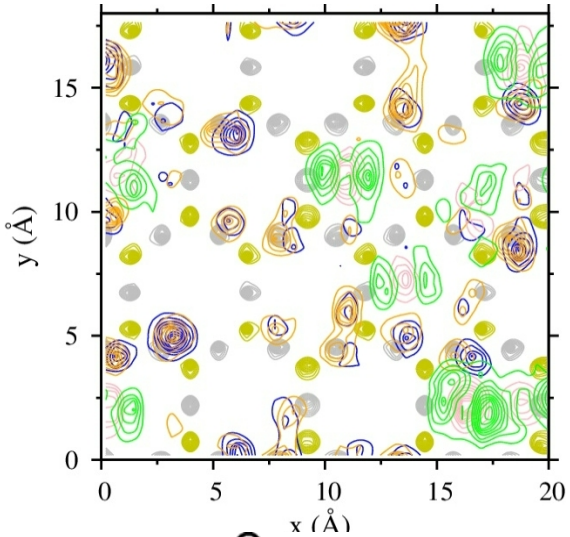

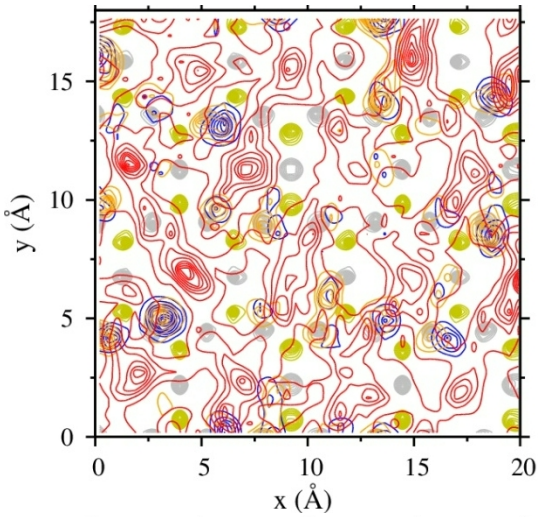

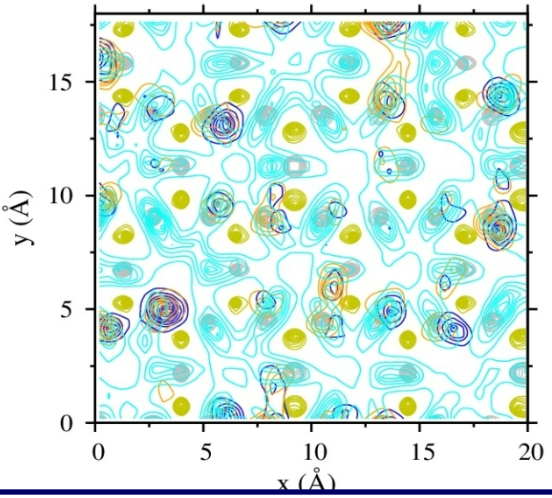

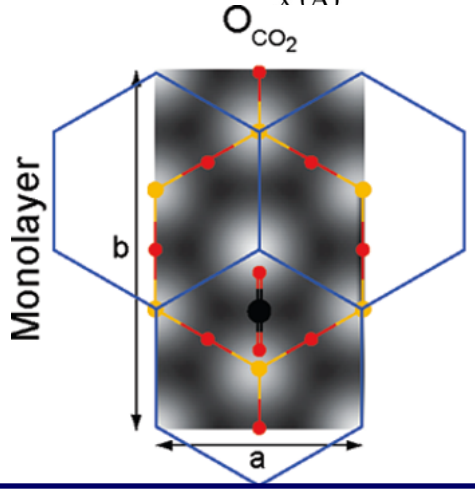

Na^+ (Blue & Orange)

O_{H2O}, H_{H2O}

C_{CO2}, O_{CO2}

Si, O_b (Surface atoms)

- Simulations confirm p orientations for CO_2 molecules
- Adsorbed aboye O_b atoms through O_{CO2}
- Mostly *slipped* geometry a less *T–shaped* configuration for CO_2 molecules

Botan et al., *J.Phys.Chem.C*, 2010, **114**, 14962-14969

Loganathan et al., *J.Phys.Chem.C*, 2017, **121**, 24527-2454; 2018, **122**, 23460-23469; 2018, **122**, 4391-4402

Molecular Models for the Intercalation of Methane Hydrate Complexes in Montmorillonite Clay

Methane hydrate intercalate structures with different interlayer cations

- Na-, K-, Ca-, and Mg-montmorillonite intercalated with CH_4 and H_2O.
- Simulated XRD patterns exhibit basal (001) *d* -values ranging from 23 Å to 24 Å.

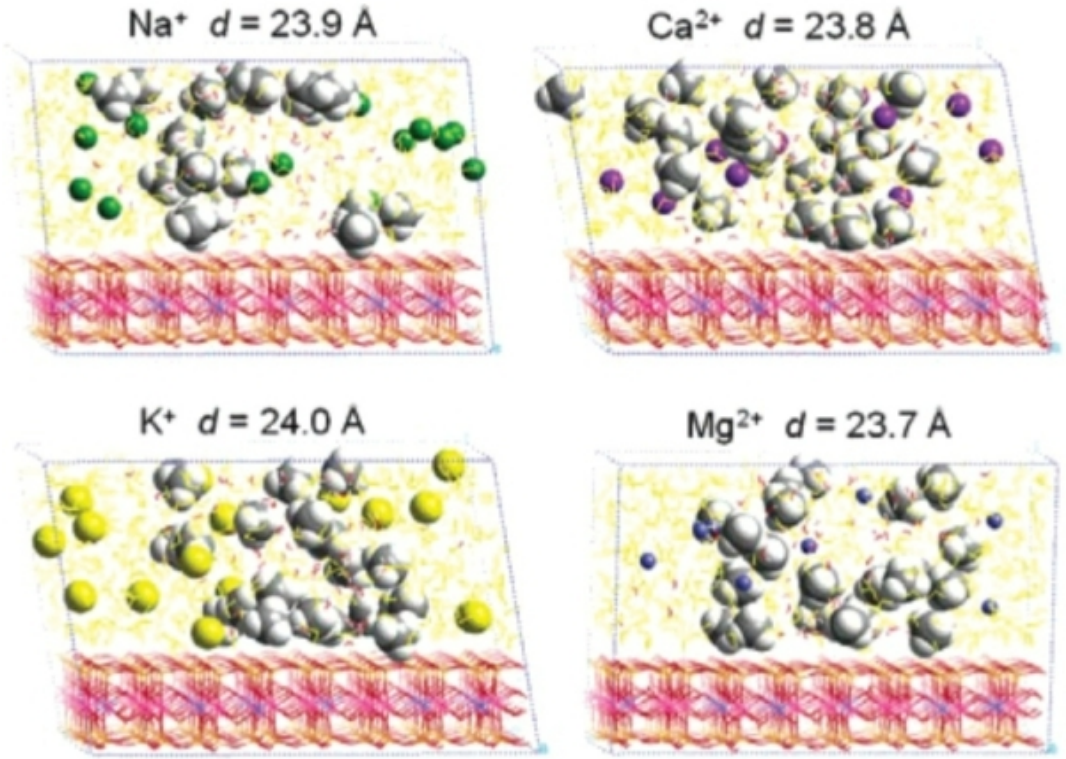

Cygan et al., *J.Phys.Chem. B*, 2004, **108**, 15141-15149

- Quantitative analysis of the C-C, O-O, and C-O RDFs indicate an interlayer structure that is different from the bulk methane hydrate and from methane in aqueous solution.
- Some order of the CH_4 hydrate structure is preserved in the interlayer and is related to the formation of methane clathrate structures with H_2O and the clay surfaces forming an H-bonded network in the interlayer.
- MD simulation results support experimental observations of a stable methane hydrate intercalate with Na-montmorillonite.

Clay Particle Edges: Special Adsorption Sites

Aggregate of clay particles

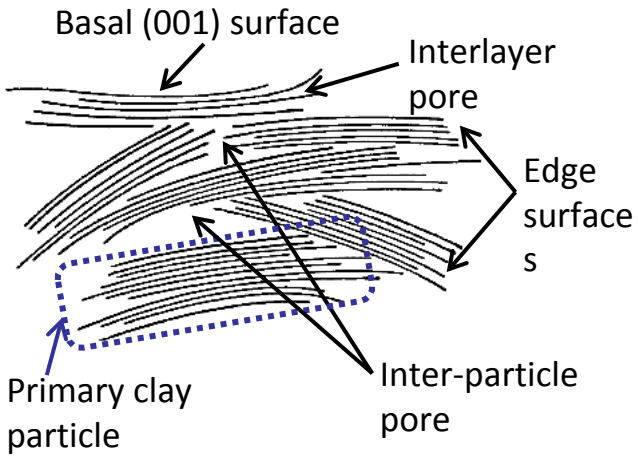

- Basal (001) surfaces and interlayers are extensively studied; their properties are reasonably well known
- Clay edges have received much less attention yet
- Ab initio (quantum) MD is a direct answer, but it is very expensive computationally
- AIMD ⇒ ~n×100 atoms; ~15×15×15 Å^3; t ~10-50 ps

S.V.Churakov, *Geochim. Cosmochim. Acta*, **71**, 1130-1144 (2007)
X. Liu et al., *Geochim. Cosmochim. Acta* (2012, 2013, 2014, 2015)
S. Tazi et al., *Geochim. Cosmochim. Acta*, **94** 1-11 (2012)

ClayFF Parametrization for Clay Edges

New special ClayFF bending terms for Mg-O-H, Al-O-H, and Si-O-H

$$U_{\text{ClayFF-MOH}} = U_{\text{ClayFF-orig}} + U_{\text{M-O-H}} = U_{\text{ClayFF-orig}} + k\,(\theta - \theta_0)^2$$

k and θ_0 have to minimize the differences between DFT and ClayFF-MOH results

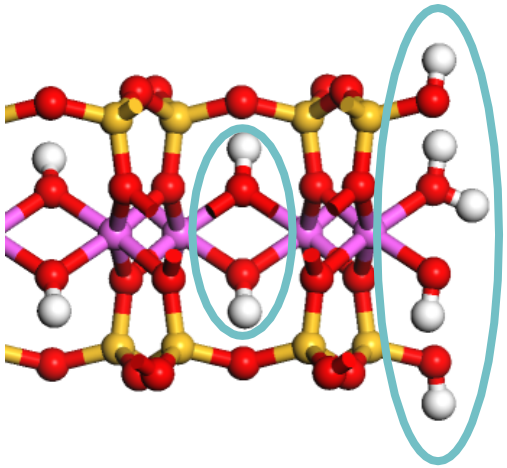

Pouvreau, Greathouse, Cygan, Kalinichev, *J.Phys.Chem.C*, 2017, **121**, 14757-14771; 2019, **123**, 11628–11638

Brucite edge: ∠Mg-O-H and $\overrightarrow{OH}$

∠Mg-O-H distribution

- DFT
- ClayFF-orig
- ClayFF-MOH:
  k_{MgOH} = 6 kcal·mol^{-1}·rad^{-2}
  k_{AlOH} = 15 kcal·mol^{-1}·rad^{-2}
- $\theta_{0\,MOH}$ = 100°
- $\theta_{0\,MOH}$ = 110°
- $\theta_{0\,MgOH}$ = 120°; $\theta_{0\,AlOH}$ = 116°

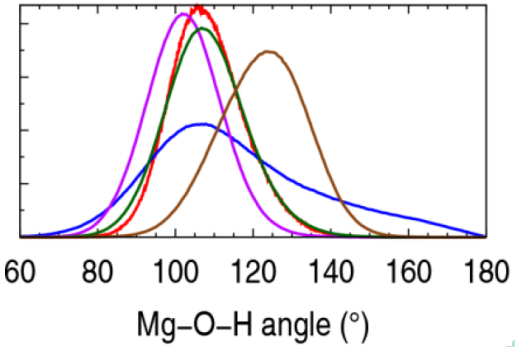

$\overrightarrow{OH}$ distribution in *xz* plane

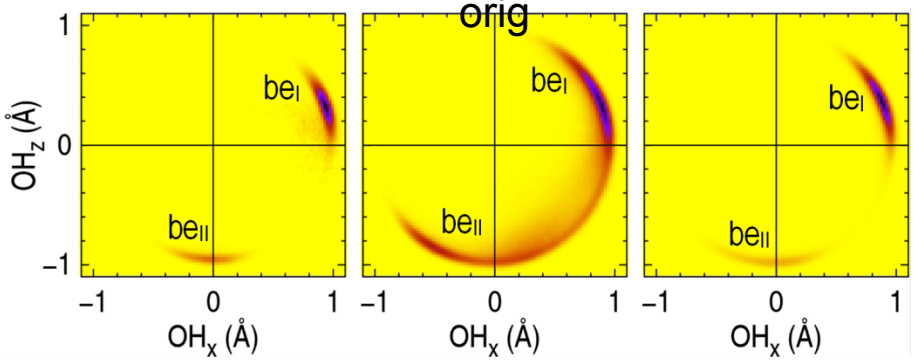

*θ_0 = 110°; k_{MgOH} = 6 kcal·mol^{-1}·rad^{-2}

- Narrowing of ∠Mg-O-H and $\overrightarrow{OH}$ distributions

M.Pouvreau, J.A.Greathouse, R.T.Cygan, A.G.Kalinichev, *J.Phys.Chem.C*, 2017, **121**, 14757-14771

Gibbsite Edge: ∠Al-O-H and $\overrightarrow{OH}$

∠Al-O-H distribution

- DFT
- ClayFF-orig
- ClayFF-MOH:
  k_{MgOH} = 6 kcal·mol^{-1}·rad^{-2}
  k_{AlOH} = 15 kcal·mol^{-1}·rad^{-2}
- $\theta_{0\,MOH}$ = 100°
- $\theta_{0\,MOH}$ = 110°
- $\theta_{0\,MgOH}$ = 120°; $\theta_{0\,AlOH}$ = 116°

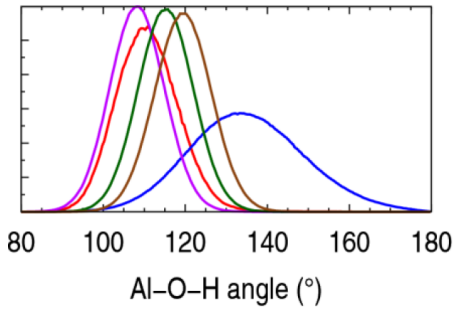

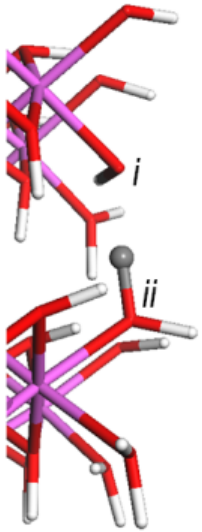

$\overrightarrow{OH}$ distribution of OH groups in *xz* plane

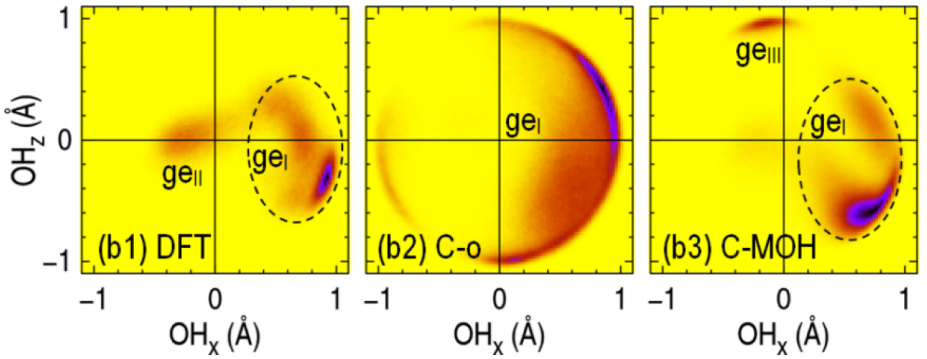

* θ_0 = 110°; k_{MgOH} ~ 15 kcal·mol^{-1}·rad^{-2}

- Narrowing of ∠Al-O-H and $\overrightarrow{OH}$ distributions
- ∠Al-O-H: both θ_0=100° and θ_0=110° are close enough to DFT results
- DFT MD: observed proton transfers between OH and OH_2 groups

M.Pouvreau, J.A.Greathouse, R.T.Cygan, A.G.Kalinichev, *J.Phys.Chem.C*, 2017, **121**, 14757-14771

Kaolinite Edge: ∠Si-O-H and $\overrightarrow{OH}$

∠Si-O-H distribution

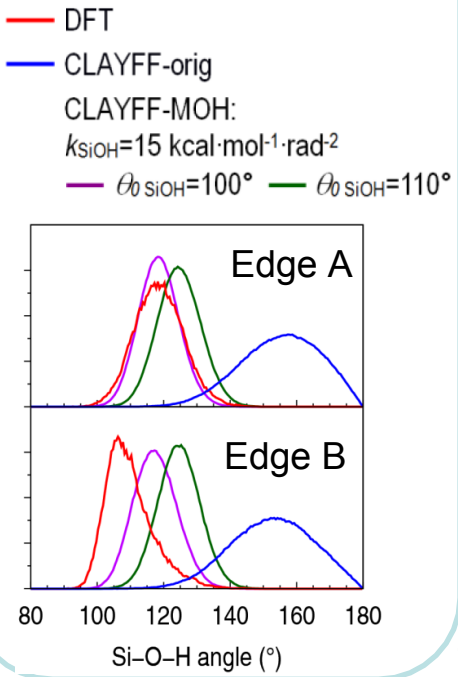

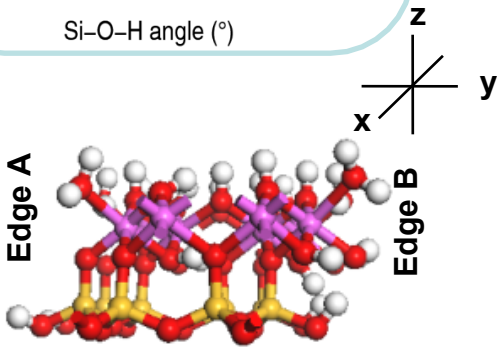

$\overrightarrow{OH}$ distribution of OH groups in *yz* plane for edge A

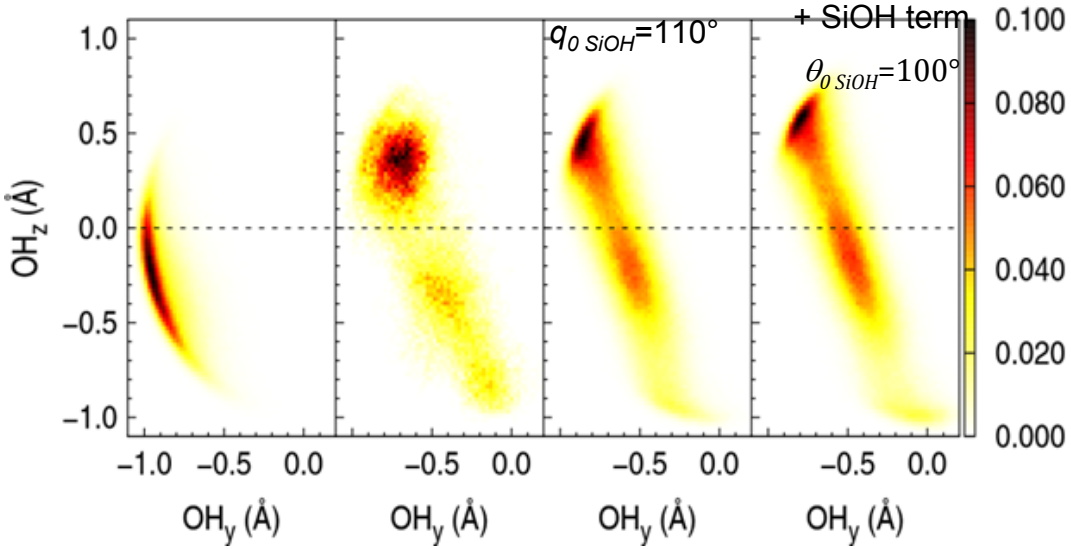

- $\theta_{0\ AlOH}$= 110°; k_{AlOH} =k_{SiOH} = 15 kcal·mol^{-1}·rad^{-2}
- $\theta_{0\ SiOH}$= 100° better than $\theta_{0\ SiOH}$= 110° on both edges
- $\overrightarrow{OH}$ distribution not affected with both values of θ_0

M.Pouvreau et al., *J.Phys.Chem.C*, 2019, **123**, 11628–11638

O-H Librational (M-O-H Bending) Spectra

- DFT
- CLAYFF-orig
- CLAYFF-MOH:
  k_{MgOH} = 6 kcal·mol^{-1}·rad^{-2}
  k_{AlOH} = k_{SiOH} 15 kcal·mol^{-1}·rad^{-2}
- $\theta_{0\ MOH}$ = 100°
- $\theta_{0\ MOH}$ = 110°

- Fourier Transform of the velocity autocorrelation function:

$$P(\nu) = \int \langle \dot{\boldsymbol{r}}(\tau) \cdot \dot{\boldsymbol{r}}(t+\tau) \rangle_\tau \, e^{-i\omega t} \, dt$$

- We consider the velocity of the H atoms of O-H groups
  → $\bar{\nu}$ < 1500 cm^{-1}: O-H libration

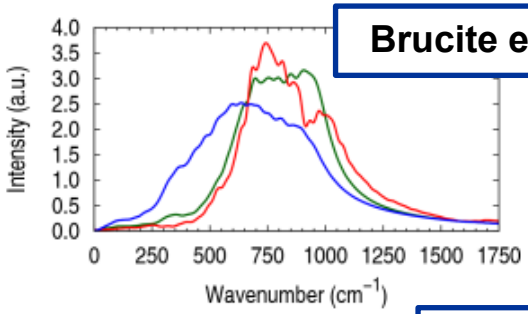

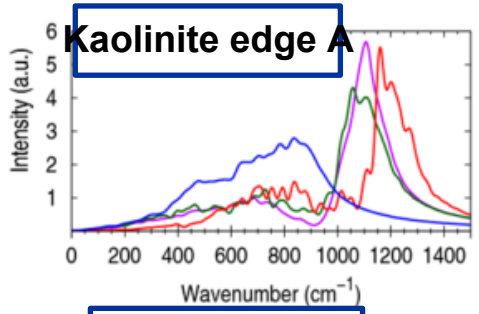

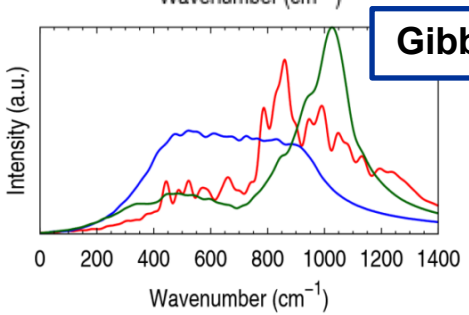

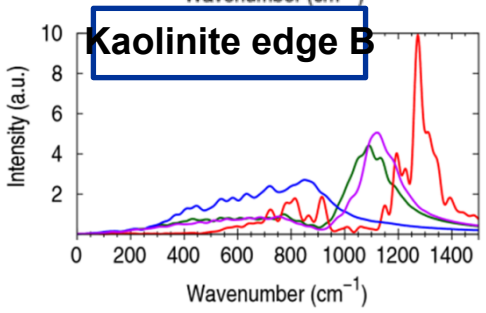

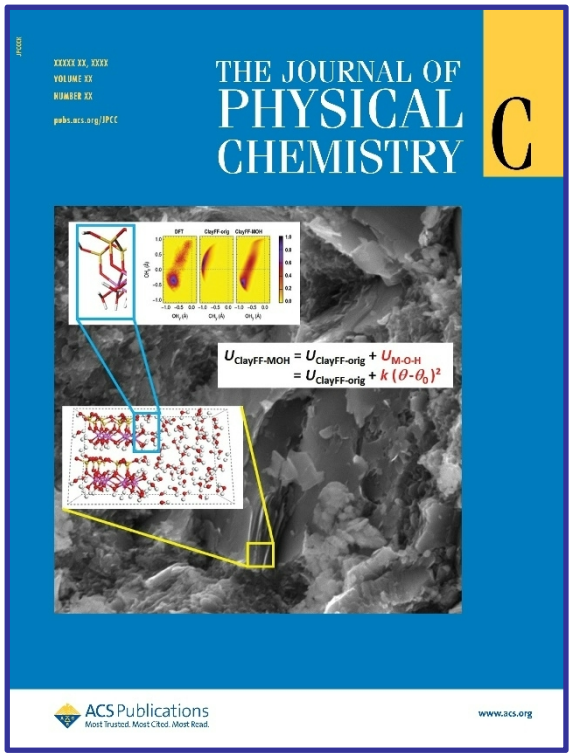

- Spectra shifted of 250 to 600 cm^{-1} and narrowed
- Kaolinite: as expected not much difference between q_0=100° and q_0=110°

M.Pouvreau, J.A.Greathouse, R.T.Cygan, A.G.Kalinichev
J.Phys.Chem.C, 2019, **123**, 11628–11638

THE JOURNAL OF PHYSICAL CHEMISTRY C
A JOURNAL OF THE AMERICAN CHEMICAL SOCIETY
pubs.acs.org/JPCC
Review Article

Advances in Clayff Molecular Simulation of Layered and Nanoporous Materials and Their Aqueous Interfaces

Randall T. Cygan, Jeffery A. Greathouse,* and Andrey G. Kalinichev

Cite This: J. Phys. Chem. C 2021, 125, 17573−17589
Read Online

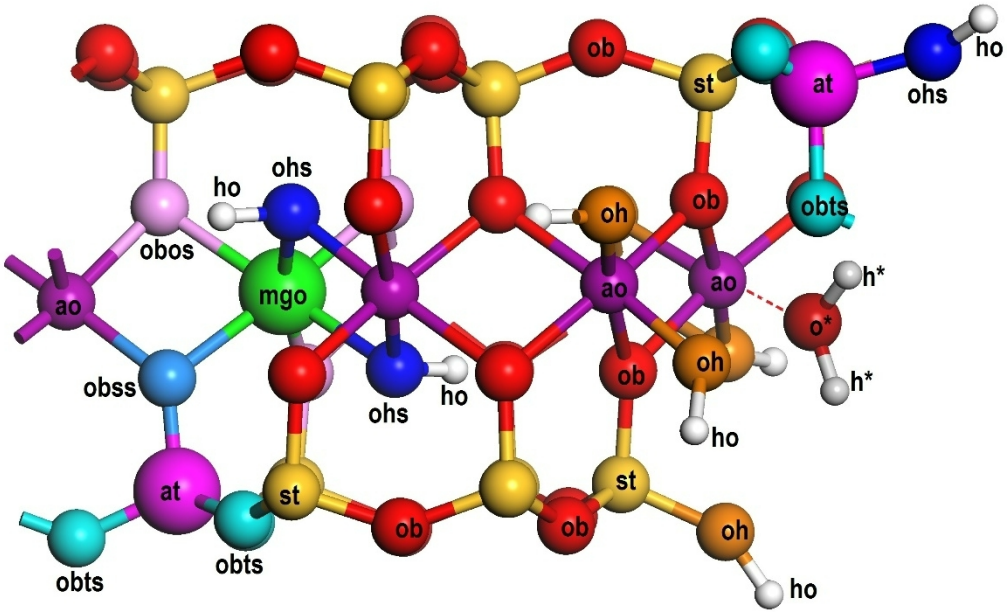

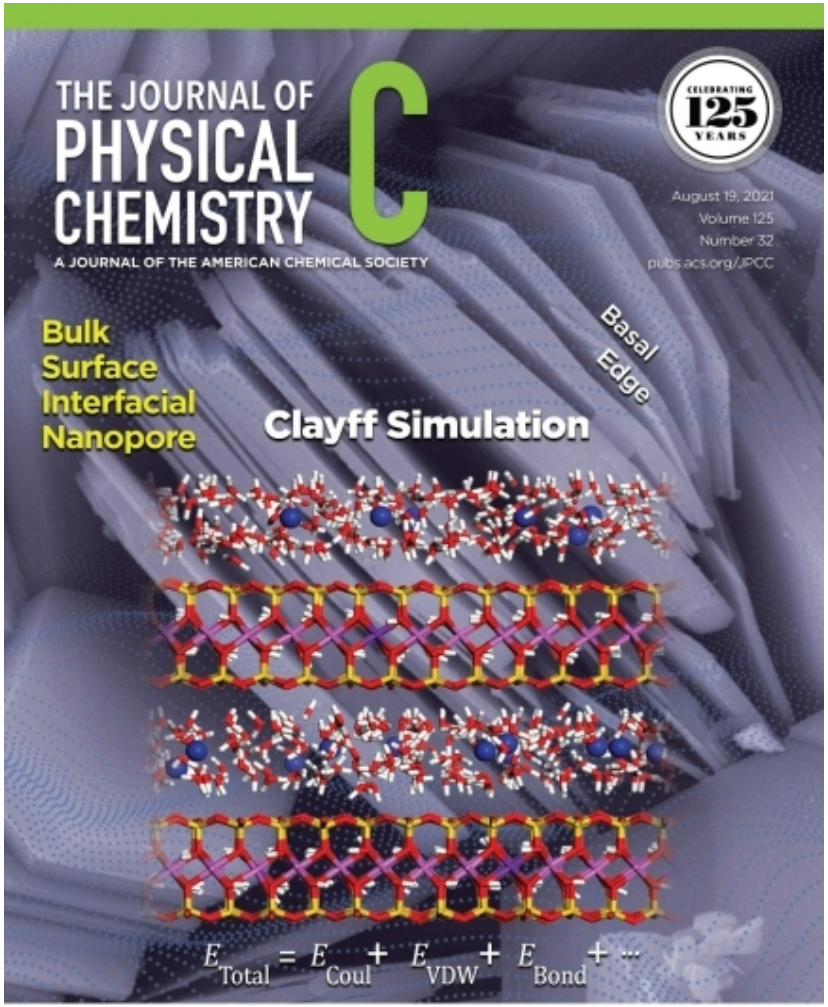

Next: Adsorption at the Particle Edges and Mesoscale Modeling of Nanoparticle Aggregates

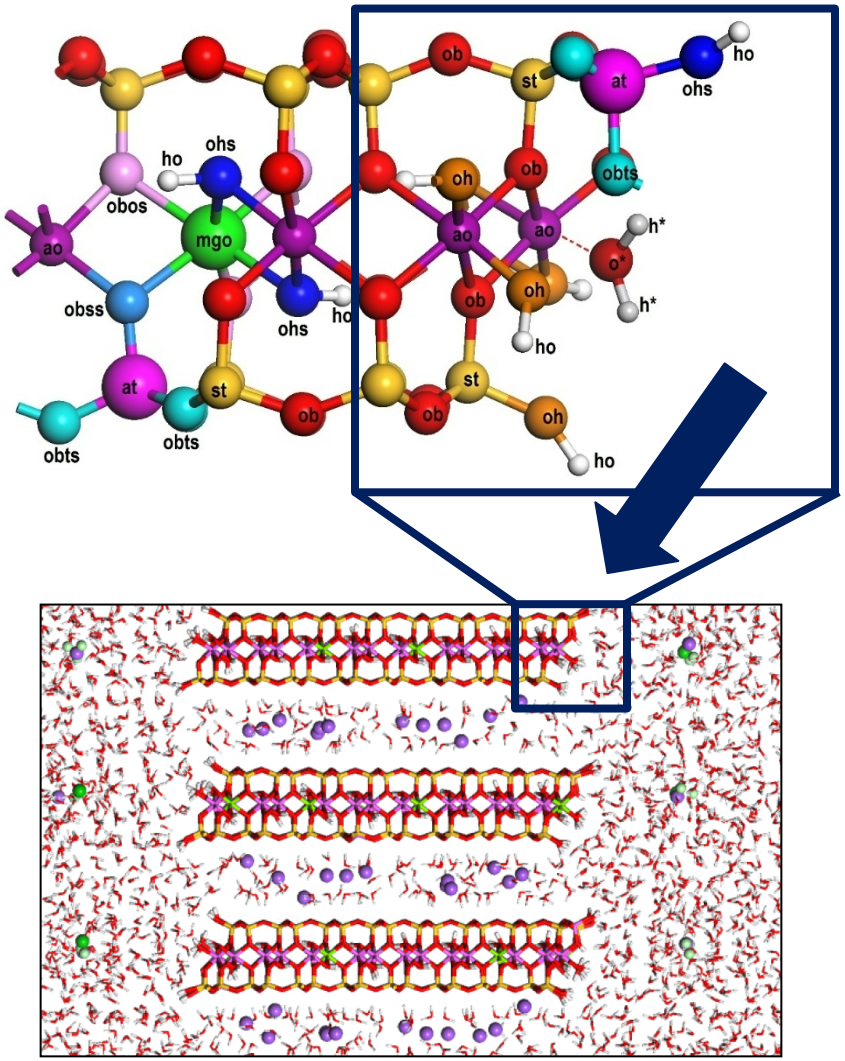

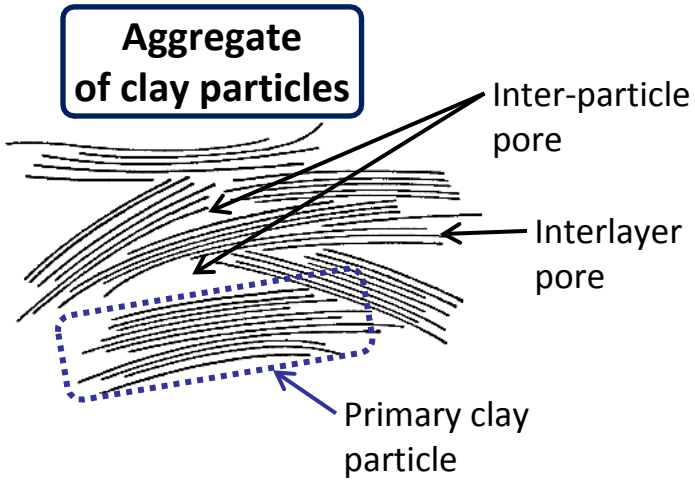

Energetics and Mechanism of Clay and Swelling (I)

THE JOURNAL OF PHYSICAL CHEMISTRY Letters

Letter

Cite This: J. Phys. Chem. Lett. 2019, 10, 3704–3709

pubs.acs.org/JPCL

Revealing Transition States during the Hydration of Clay Minerals

Tuan A. Ho,* Louise J. Criscenti, and Jeffery A. Greathouse

Geochemistry Department, Sandia National Laboratories, Albuquerque, New Mexico 87185, United States

Supporting Information

ABSTRACT: A molecular-scale understanding of the transition between hydration states in clay minerals remains a challenging problem because of the very fast stepwise swelling process observed from X-ray diffraction (XRD) experiments. XRD profile modeling assumes the coexistence of multiple hydration states in a clay sample to fit the experimental XRD pattern obtained under humid conditions. While XRD profile modeling provides a macroscopic understanding of the heterogeneous hydration structure of clay minerals, a microscopic model of the transition between hydration states is still missing. Here, for the first time, we use molecular dynamics simulation to investigate the transition states between a dry interlayer, one-layer hydrate, and two-layer hydrate. We find that the hydrogen bonds that form across the interlayer at the clay particle edge make an important contribution to the energy barrier to interlayer hydration, especially for initial hydration.

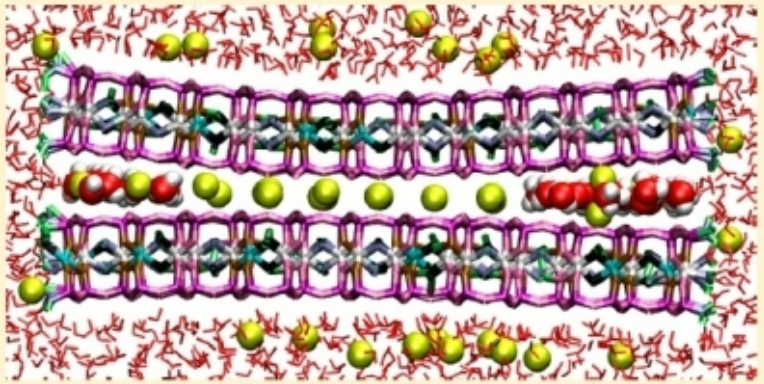

Energetics and Mechanism of Clay and Swelling (II)

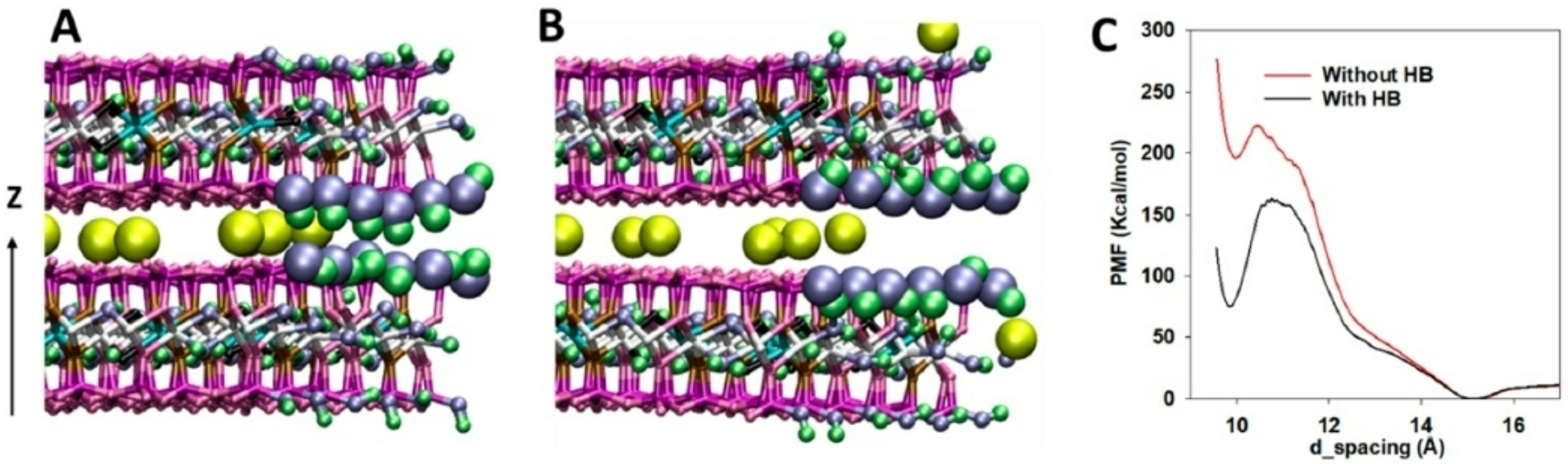

- Edge H-bonds between TOT layers in the dry state act like a gate, preventing the passage of water molecules and ions into the interlayer
- Swelling process begins by breaking those H-bonds so that H_2O molecules can diffuse into the interlayer
- It is possible that proton transfer could significantly affect the mechanism and energy differences between hydration states

Ho et al., *J.Phys.Chem.Lett.*, **10,** 3704-3709 (2019)

Shale Oil and Gas Extraction

Shale formations are characterized by a small porosity and low permeability* that trap hydrocarbons in host rocks. Hydraulic fracturing increases the extremely low permeability of shale rocks, enabling the economic production of shale gas and oil**.

Schematic representation of shale gas extraction***

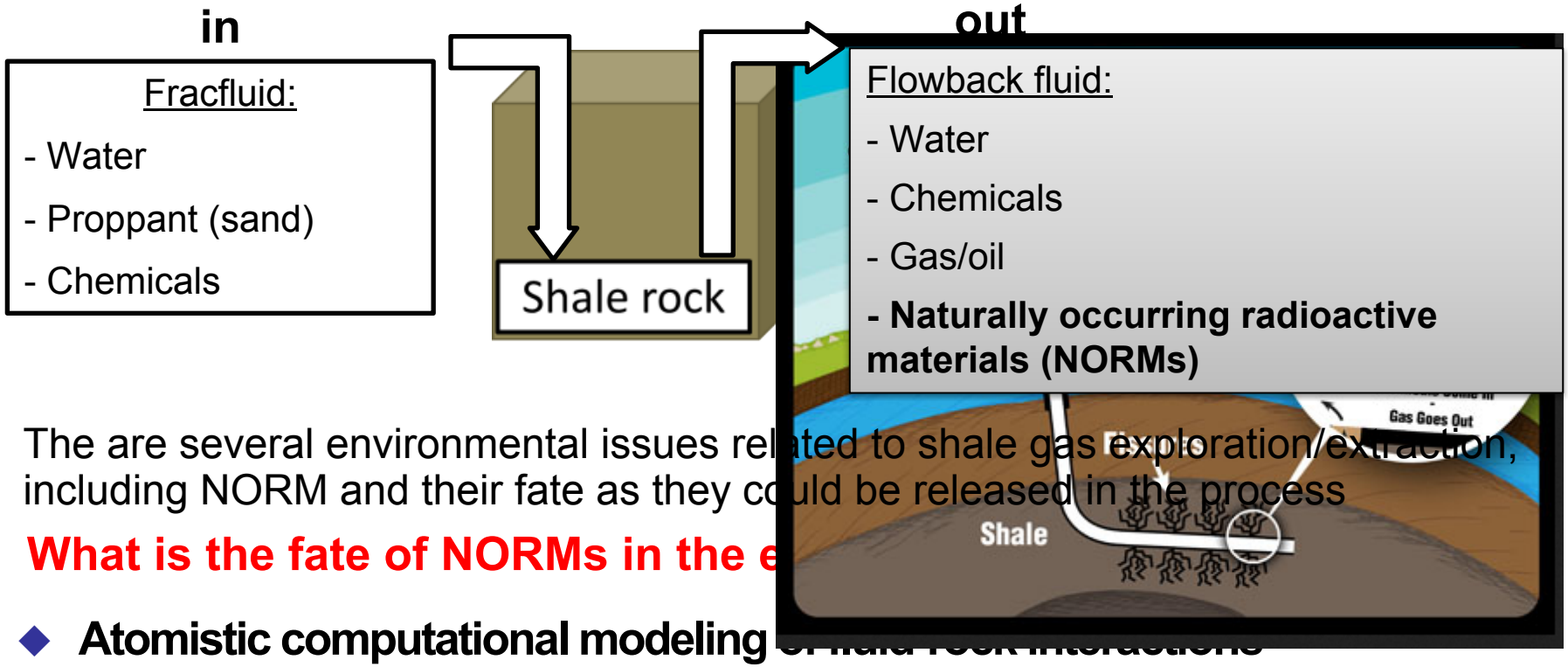

The are several environmental issues related to shale gas exploration/extraction, including NORM and their fate as they could be released in the process

What is the fate of NORMs in the e

- **Atomistic computational modeling of fluid-rock interactions**

* Ho TA, Striolo A. *AIChE Journal*, **61**, 2993 (2015)
** Yethiraj A, Striolo A. *J. Phys. Chem. Lett.*, **4**, 687 (2013)
*** http://www.virtualmuseum.ca/edu/ViewLoitDa.do?method=preview&lang=EN&id=25977

(010) Montmorillonite Edge: Interlayer *vs* Interface Adsorption of NORM Cations

- All cations are more stable in the interlayer compared to the interfacial region
- The associated average free energy gain are as follows :
  - **~10 kJ/mol for Na^+**
  - **~25 kJ/mol for Sr^{2+}**
  - **~19 kJ/mol for Ba^{2+}**
- The energy gain when Na^+ enters the interlayer region is almost doubled for Sr^{2+} and Ba^{2+}: 1 Sr^{2+}/Ba^{2+} for 2 Na^+ ions.
- This is consistent with our statistical analyses showing that ~70% of Sr^{2+}/Ba^{2+} initially present in the interfacial region migrate in the interlayers during the simulations
- There are noticeable energy barriers at the (010) edge for Sr^{2+}/Ba^{2+} to enter the MMT interlayers

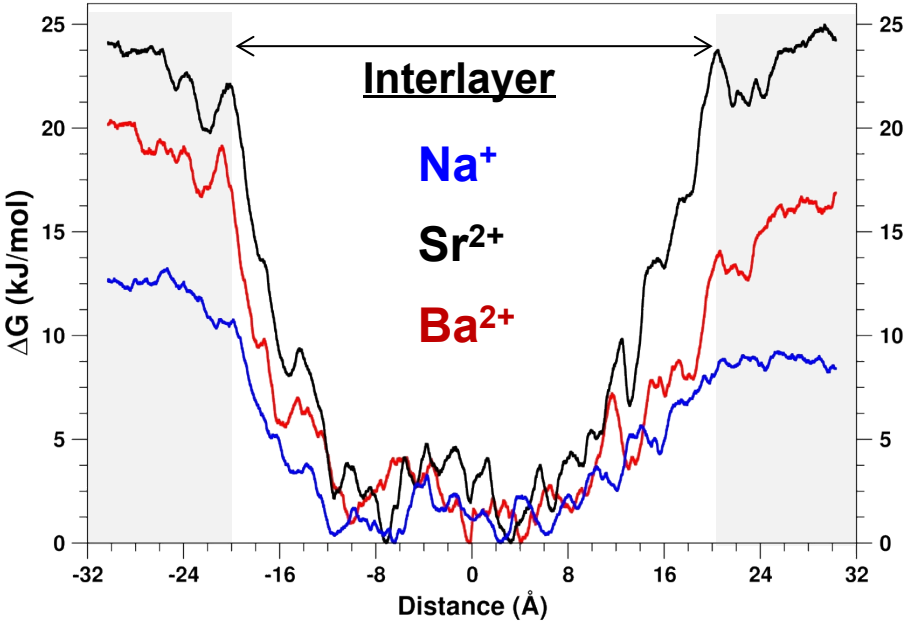

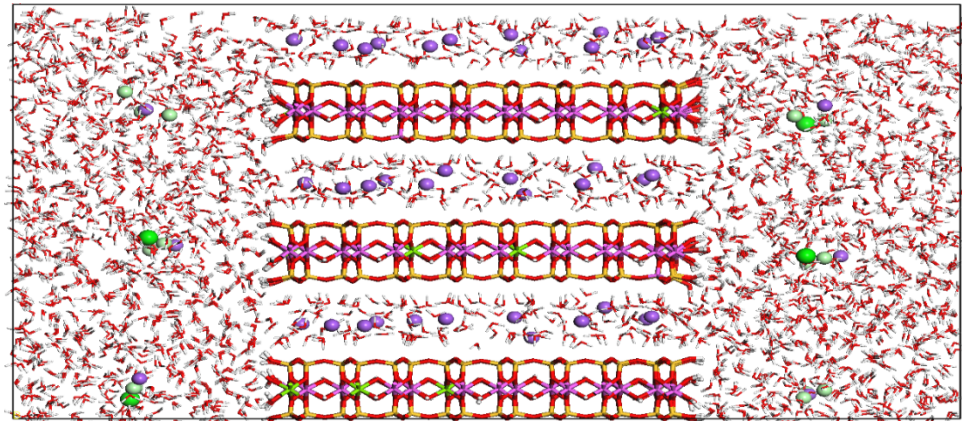

B.F.Ngouana et al., *J.Phys.Chem.C*, 2022, in prep.

CH_4/CO_2 Partitioning in Clay Nano- and Meso-Pores: Molecular Dynamics Modeling with Constant Reservoir Composition

N.Loganathan, G.M.Bowers, B.F.Ngouana-Wakou, A.G.Kalinichev, R.J.Kirkpatrick, O.Yazaydin
PCCP, **21**, 6917-6924 (2019); *JPCC*, **124,** 2490−2500 (2020)

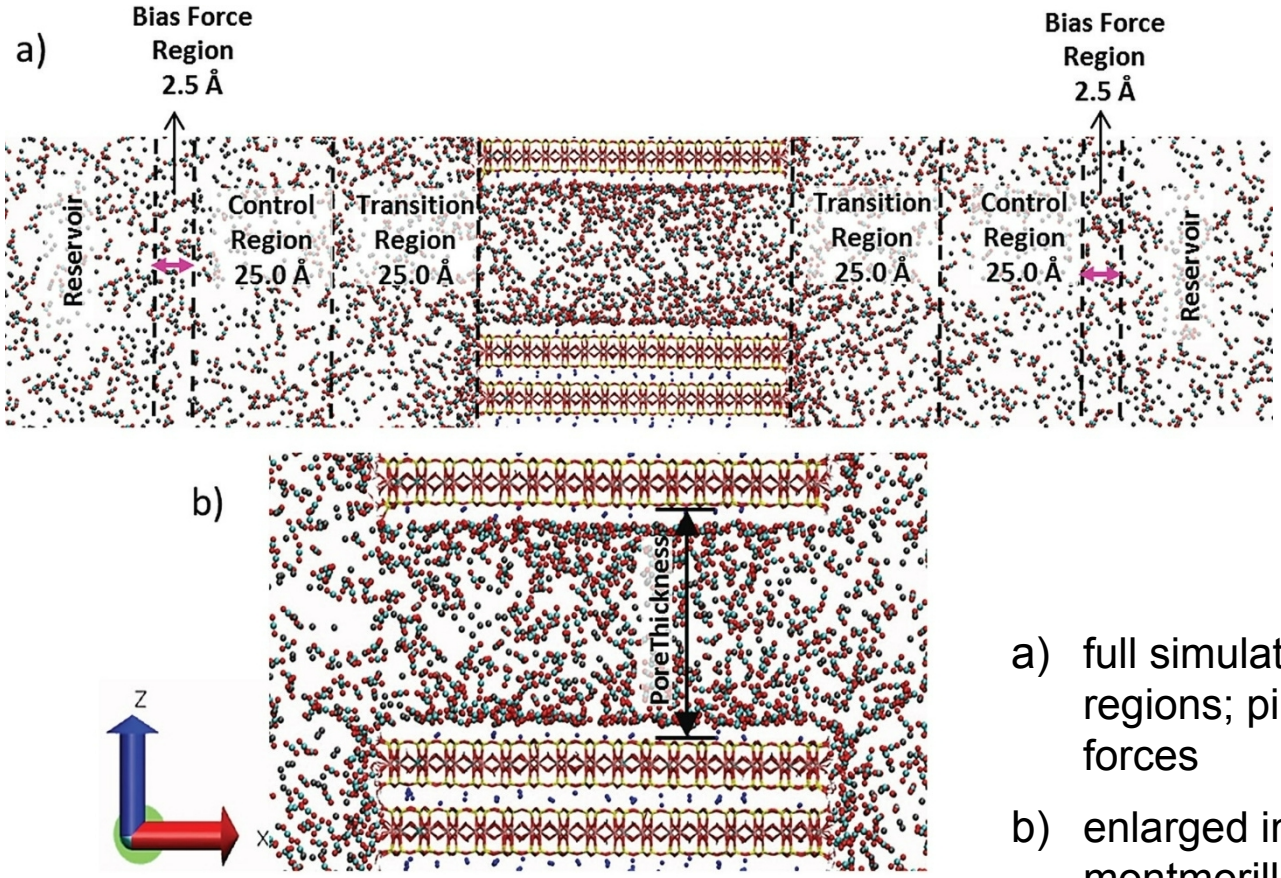

Scheme of the simulation cells used in the constant reservoir composition molecular dynamics, CRC-MD calculations of CO_2/CH_4 partitioning into pores bounded by montmorillonite basal surfaces

a) full simulation cell showing the different regions; pink arrows represent bias forces

b) enlarged image of the silt-like pore and montmorillonite T-O-T layers

THE JOURNAL OF PHYSICAL CHEMISTRY C

pubs.acs.org/JPCC Article

Large-Scale Molecular Dynamics Simulation of the Dehydration of a Suspension of Smectite Clay Nanoparticles

Thomas R. Underwood* and Ian C. Bourg*

Cite This: *J. Phys. Chem. C* 2020, 124, 3702–3714

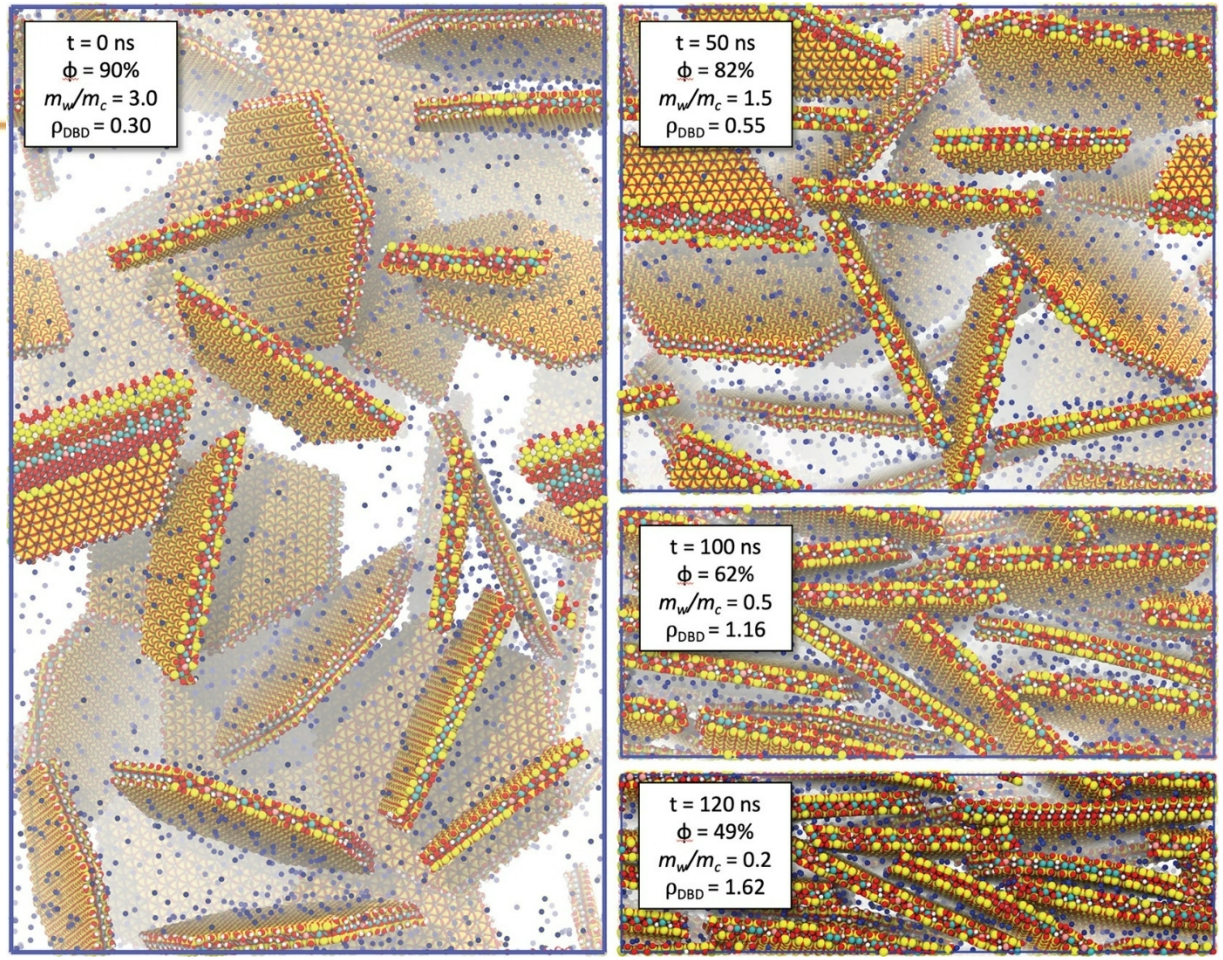

ADVANCED MATERIALS
www.advmat.de
Adv. Mater. **2015**, *27*, 966–984
Materials Views
www.MaterialsViews.com

Chemically Specific Multiscale Modeling of Clay–Polymer Nanocomposites Reveals Intercalation Dynamics, Tactoid Self-Assembly and Emergent Materials Properties

*James L. Suter, Derek Groen, and Peter V. Coveney**

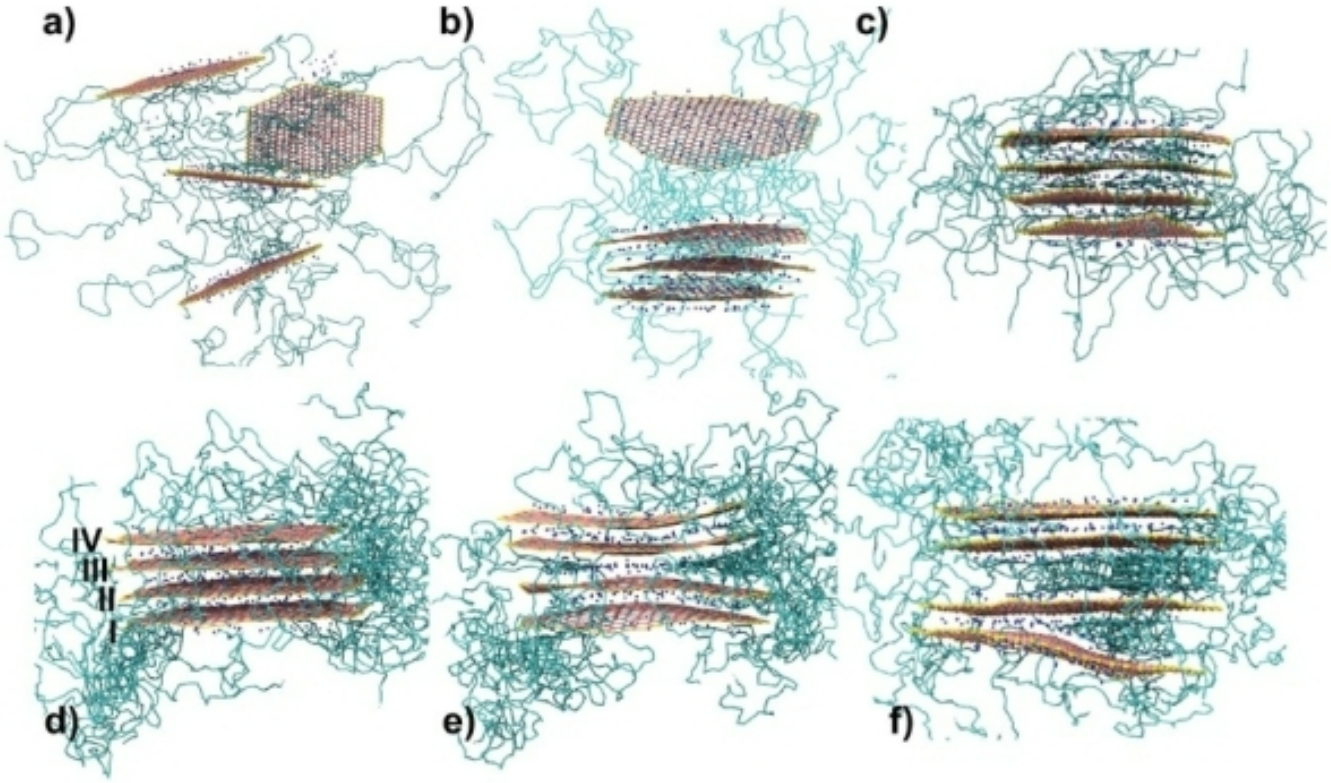

Multiscale Problems & Approaches (I)

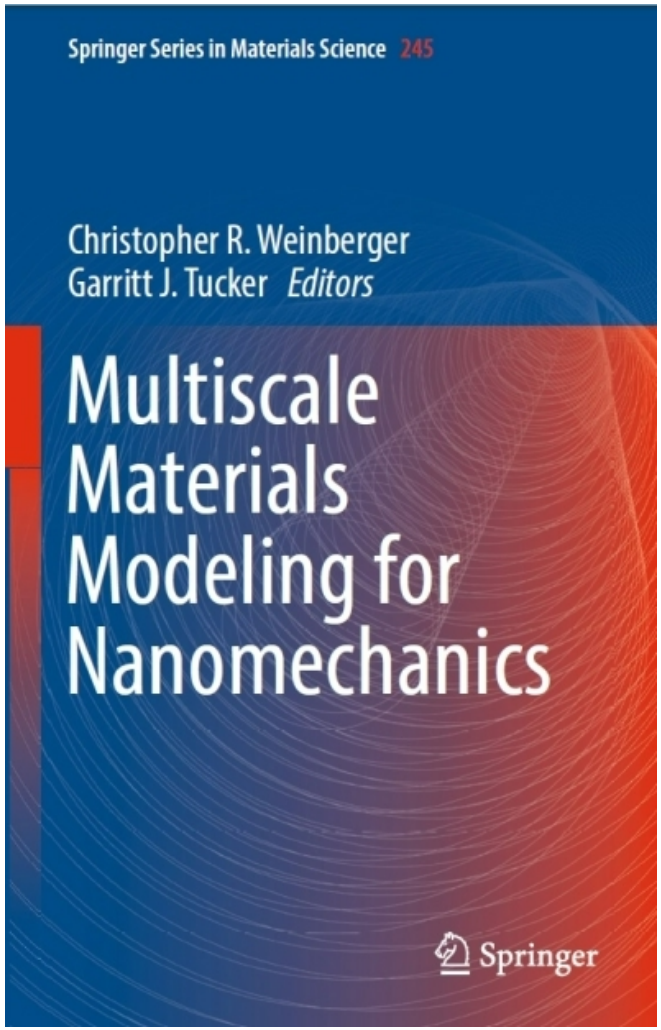

Weinberger, C. R.; Tucker, G. J.(Eds.) *Multiscale Materials Modeling for Nanomechanics.* Springer International Publishing, 2016, 554pp.

Multiscale Problems & Approaches (II)

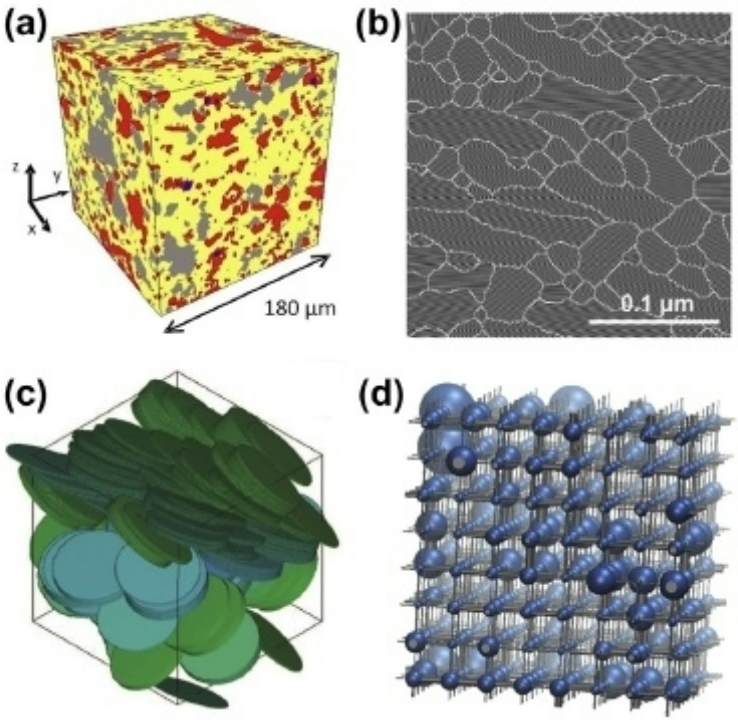

FIGURE 11.3 Models of representative elementary volume. (a) 3D mineralogical map of Callovo-Oxfordian clay obtained from X-ray tomography experiments. *(Reprinted from Robinet et al. (2012), Copyright 2012, with permission of John Wiley & Sons, Inc.)* (b) 2D grain structure used to model diffusion in montmorillonite. *(Reprinted from Churakov et al. (2014), with permission from Elsevier.)* (c) 3D packing of ellipsoids obtained using a potential of mean force from Molecular simulations. *(Reprinted from Ebrahimi et al. (2014), Copyright 2014, AIP Publishing LLC.)* (d) Pore network model *(Copyright Amaël Obliger.)*.

Marry, V.; Rotenberg, B., Upscaling Strategies for Modeling Clay-Rock Properties. In *Developments in Clay Science*, Tournassat, C.; Steefel, C. I.; Bourg, I. C.; Faïza, B., Eds. Elsevier: 2015; Vol. 6, pp 399-417.

Multiscale Problems & Approaches (III)

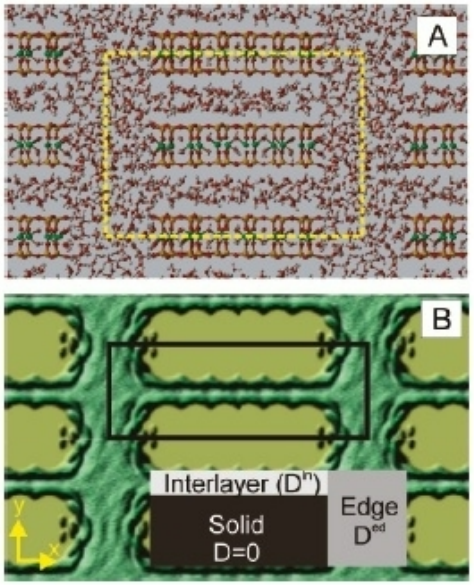

Figure 1. (A) Snapshot from MD simulations of pyrophyllite particles separated by two water layers. Oxygen, hydrogen, silica, and aluminum atoms are shown as red, gray, yellow, and green spheres, respectively. The simulation supercell is shown by the yellow dashed line. (B) A surface plot of the 2D probability density profile of water molecules from molecular dynamics simulations. Peak areas correspond to long residence times. In the overlay, light gray and gray areas indicate interlayer space and interparticle porosity, respectively, as assigned for the RW simulations. The diffusion coefficients D^{in} and D^{ed} for these pore spaces were obtained from short (200 ps) MD trajectories resident in the corresponding domains. The solid phase domain impenetrable for water is shown as a black area. The simulation cell for the RW simulations is shown by the solid black line.

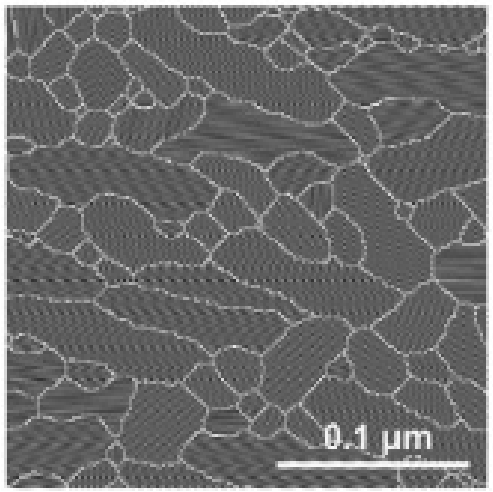

Churakov, S. V.; Gimmi, T., Up-Scaling of Molecular Diffusion Coefficients in Clays: A Two-Step Approach. *Journal of Physical Chemistry C* **2011,** *115*, 6703-6714

Multiscale Problems & Approaches (IV)

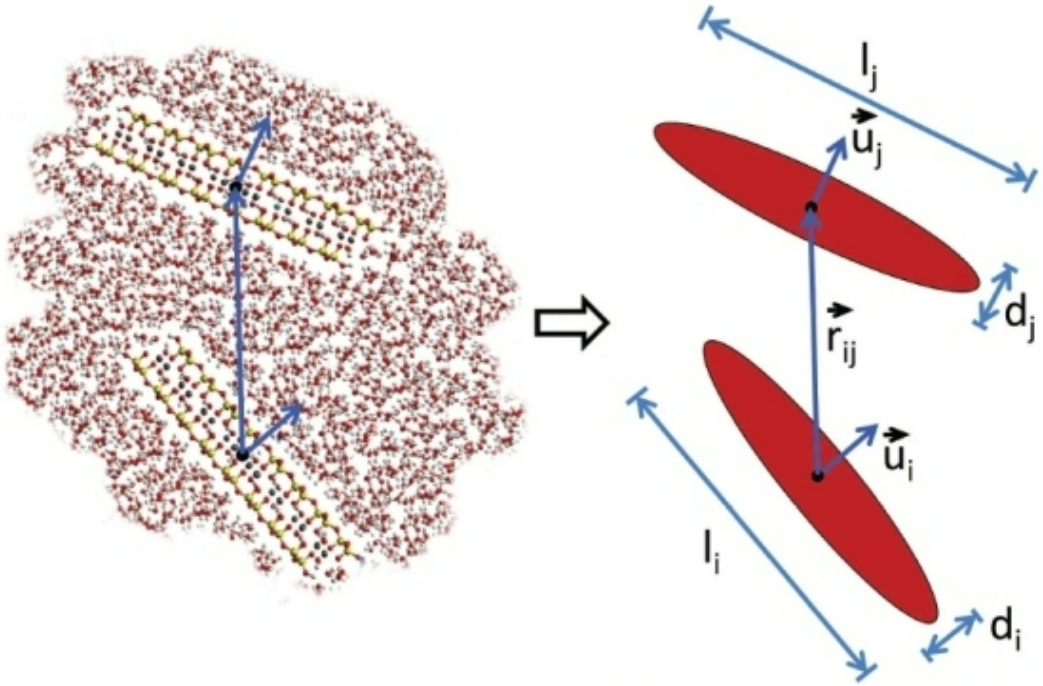

Figure 2. Interactions between two clay platelets are approximated by single-site potential functions for an ellipsoidal body (GB potential).

Ebrahimi, D.; Whittle, A. J.; Pellenq, R. J. M., Effect of polydispersity of clay platelets on the aggregation and mechanical properties of clay at the mesoscale. *Clays and Clay Minerals* **2016,** *64*, 425-437

Multiscale Problems & Approaches (V)

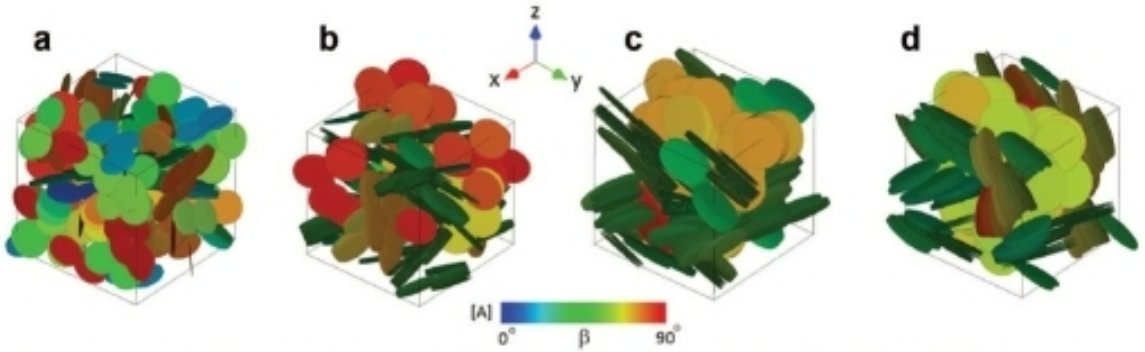

Figure 5. Examples of the final configuration of the system of particles with diameter $D = 601$ Å at pressure $P =$ (a) 1 atm; (b) 10 atm; (c) 300 atm; and (d) 800 atm. The orientations of the particles are color coded according to the β angle, the orientation of their normal vector with respect to the Z axis (colorbar A). By increasing the pressure the spectrum of colors decreased as the stack size increased and the system became more ordered. At high pressure ($P = 800$ atm), platelets started to slide against each other.

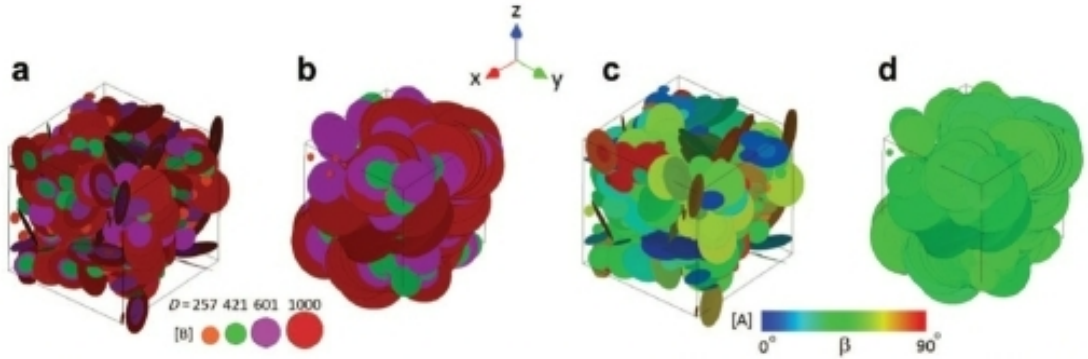

Figure 7. Examples of the final configuration of the polydisperse system of particles with diameters $D = 257, 421, 601$, and 1000 Å at pressure P, (a, c) = 1 atm, (b, d) = 800 atm. In parts a and b, particles are color coded based on their size (colorbar B) and in parts c and d they are color coded according to the β angle, the orientation of their normal vector with respect to the Z axis (colorbar A). By increasing the pressure, the spectrum of color decreases as the system becomes more ordered (see c and d).

Ebrahimi et al., Effect of polydispersity of clay platelets on the aggregation and mechanical properties of clay at the mesoscale. *Clays and Clay Minerals* **2016,** *64*, 425-437

Multiscale Problems & Approaches (VI)

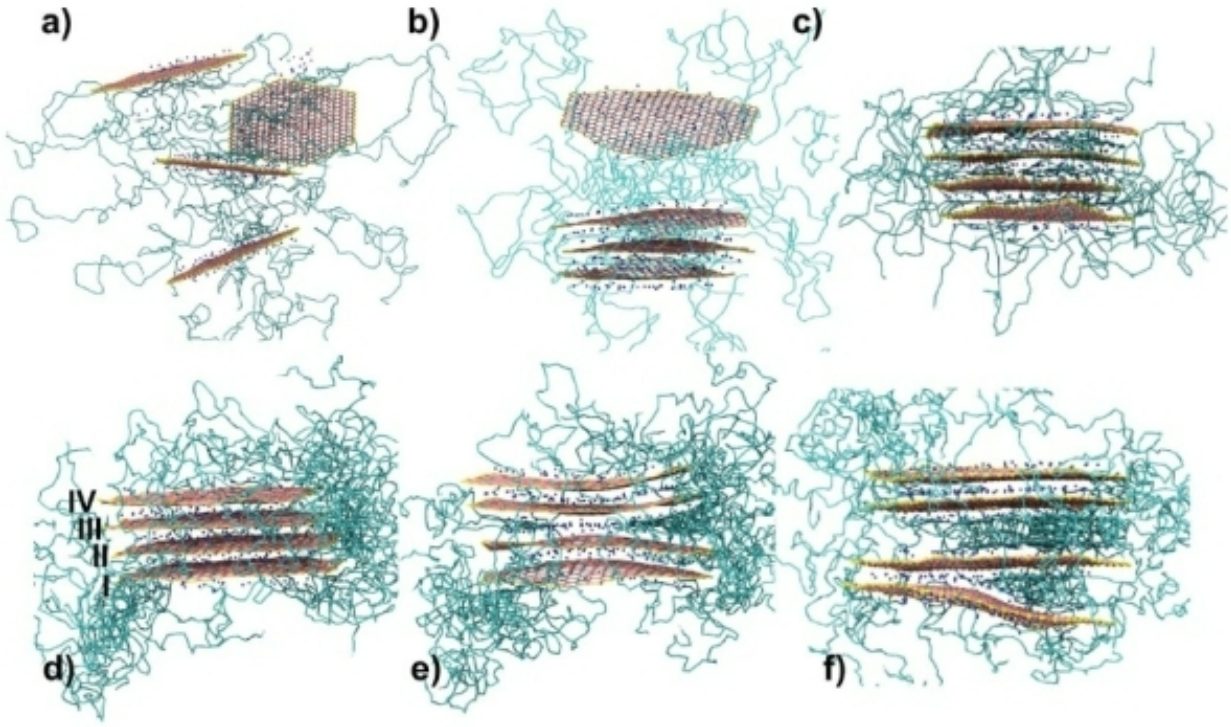

Suter, J. L.; Groen, D.; Coveney, P. V., Chemically specific multiscale modeling of clay-polymer nanocomposites reveals intercalation dynamics, tactoid self-assembly and emergent materials properties. *Advanced Materials* **2015,** *27*, 966-984

Multiscale Problems & Approaches (VII)

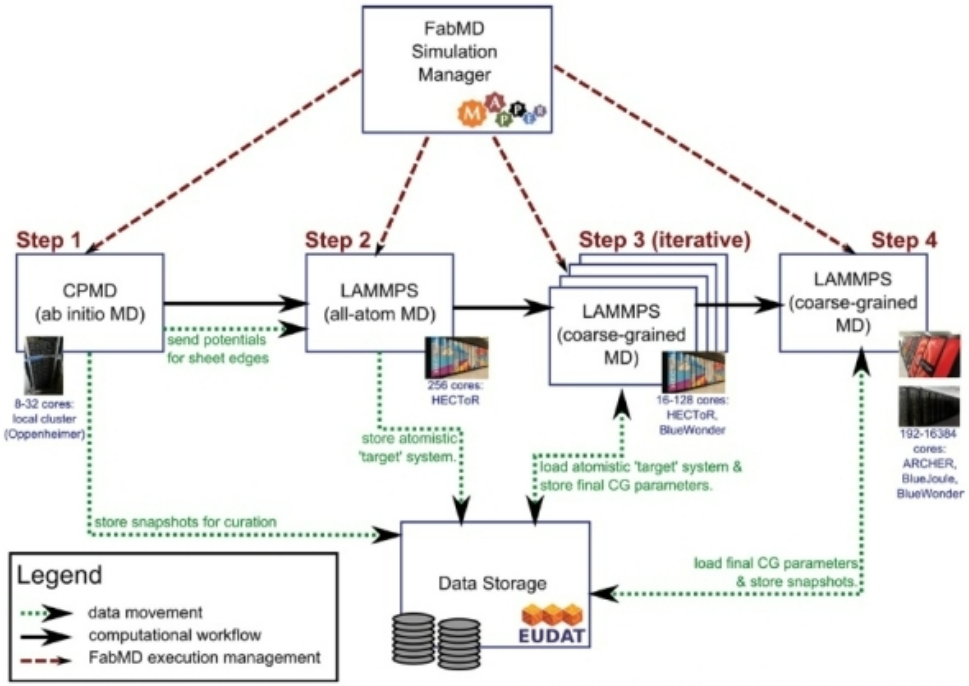

Figure 4. Overview of the computational and data workflow applied in our multiscale modeling scheme. We use the FabMD toolkit to help automate the four primary steps in our approach. These include ab initio calculations of the forces on the sheet edges (step 1, run on a departmental cluster), all-atom MD simulations to extract key distribution functions (step 2, run on a supercomputer), hundreds of small coarse-grained MD simulations performed iteratively to find the optimal parameters for the coarse-grained system (step 3, mostly run on a supercomputer), and finally the coarse-grained MD production runs (step 4, with simulations run on several different supercomputers). For each step in the workflow, we provide basic information about the HPC resources used below the description box. We use a distributed data-storage system, provided by EUDAT (http://www.eudat.eu), to facilitate the exchange of data between the different steps of the workflow and to curate the output of our simulations.

Suter, J. L.; Groen, D.; Coveney, P. V., Chemically specific multiscale modeling of clay-polymer nanocomposites reveals intercalation dynamics, tactoid self-assembly and emergent materials properties. *Advanced Materials* **2015,** *27*, 966-984

Conclusions and Outlook (I)

- ***Computational atomistic modeling*** is a powerful tool to study many nano-scale phenomena in clay mineralogy and geochemistry, complementary to other experimental physical and chemical methods already widely used to characterize properties of clays
- ***ClayFF*** is a simple but surprisingly successful force field in modeling clay-related phases, the structure and dynamics of their aqueous interfaces
- Molecular simulations can ***qualitatively, and often quantitatively, reproduce and predict*** the structure and properties clay minerals and their aqueous interfaces
- The ***ability to improve our physical understanding*** of the complex physical and chemical behavior of these systems and to unravel many fundamental atomic- and molecular-scale correlations between their structural, transport, spectroscopic, and thermodynamic properties ***is the most valuable feature of these techniques***
- We already have a very ***high degree of quantitative molecular scale understanding*** for the interfacial phenomena on the ***basal surfaces of clay minerals (001)***
- The ***role of clay particle edges*** is very important in many cases, but requires additional modeling efforts, which are also currently under way

Conclusions and Outlook (II)

- Recent modifications correct several known problems with ClayFF
- Pretty good description of the basal surfaces and interlayers of clays
- Current challenges to realistic molecular modeling of the adsorption and transport of fluids confined in clay-related materials:
  - ✓ **Compositional diversity and disorder**
  - ✓ **Structural and stacking disorder**
  - ✓ **Effects of interstratification**
  - ✓ **Effects of organics in clay nano-pores**
  - ✓ **Role of particle edges**
  - ✓ **Chemical reactivity**

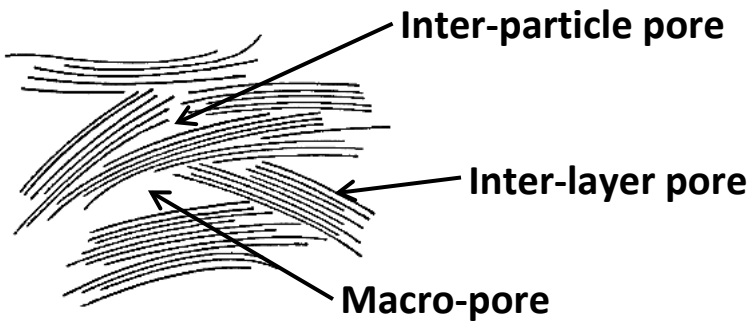

- Many of these challenges can be addressed by simply using larger (more disordered) model structures and longer simulation times with available force field parameterizations (e.g., *ClayFF*)
- Molecular modeling of fluids in multi-scale porous system is now possible
- *Ab initio* (quantum) MD / DFT approaches are computationally prohibitively expensive for large disordered systems such as clay or cement phases
- There is a clear need for a empirical reactive force field for classical simulations (*ReaxFF* ?? *Reactive ClayFF ???*)

Conclusions and Outlook (III)

- Good consistency of MD-simulated results with X-ray, NMR, INS, QENS measurements
- Simulations with larger ***more realistic and diverse models*** of reactive mineral-water interfaces are necessary
- New quantitative ***multi-scale*** approaches need to be developed
- Close ***collaboration between experimental and molecular modeling*** approaches is necessary
- New more powerful ***peta- and exa- scale supercomputing*** facilities are becoming extremely helpful in allowing to address the observed phenomena at much larger geochemically and environmentally relevant time- and length- scales

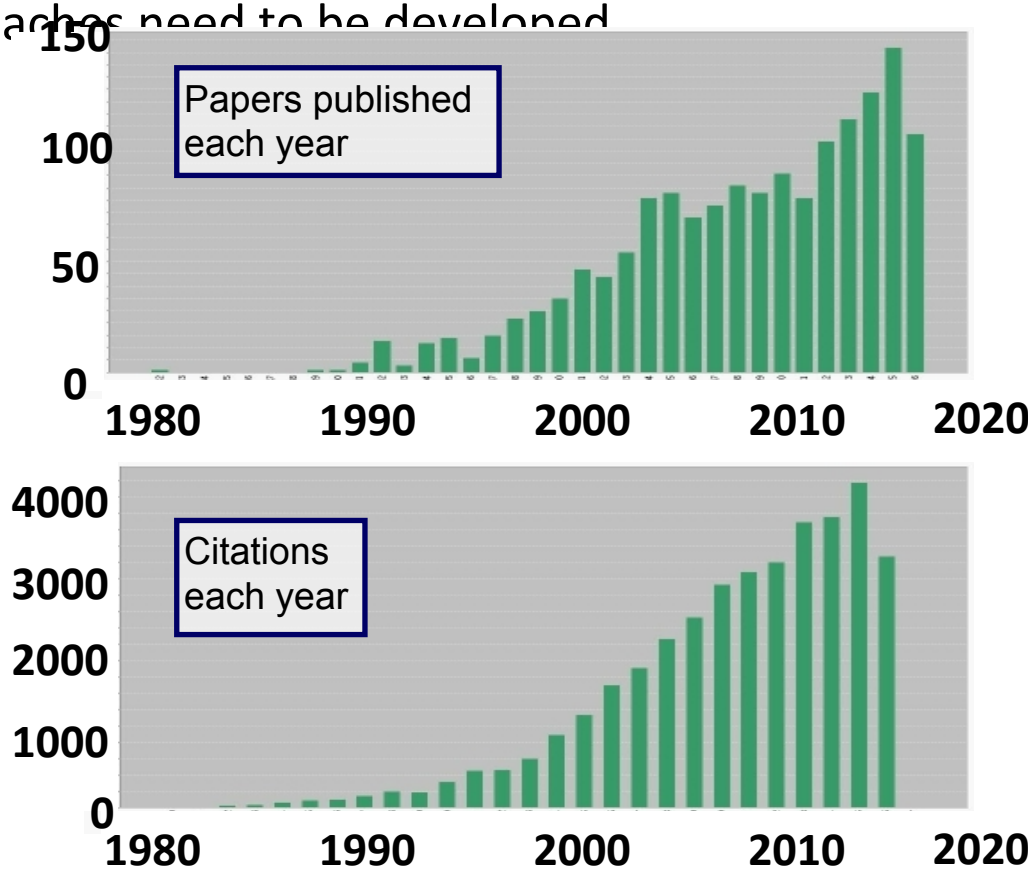

- **Bright future ahead!**

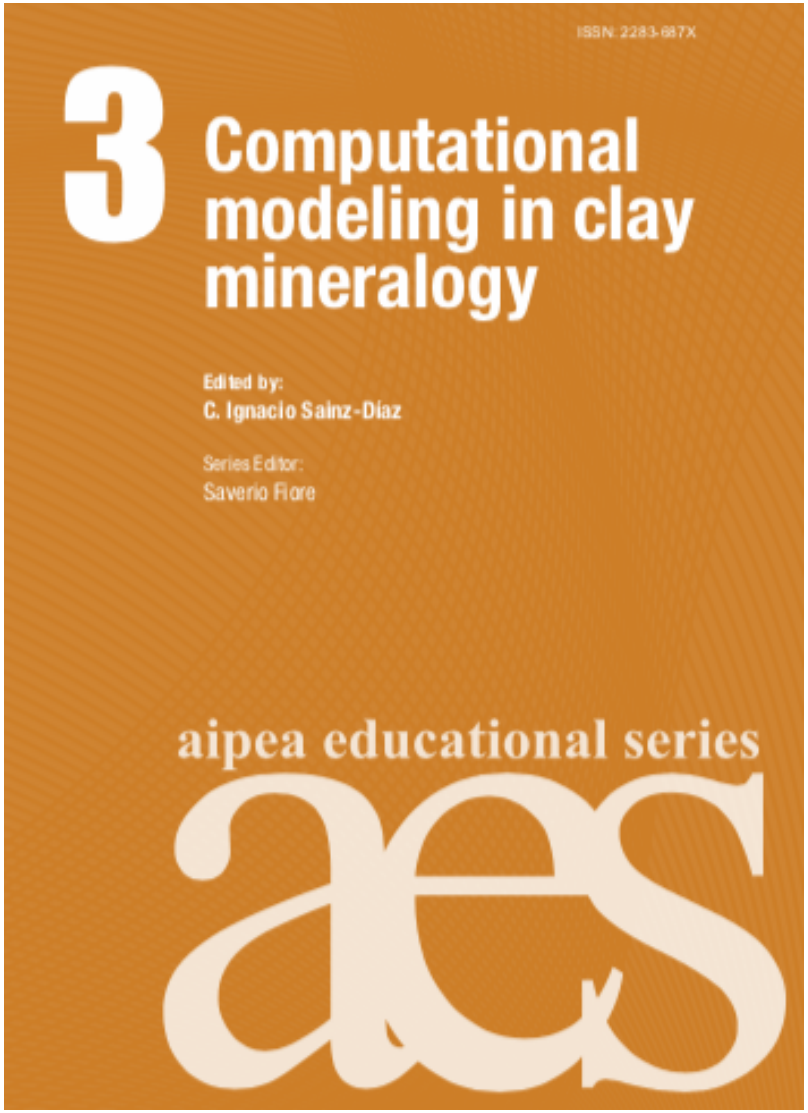

CONTENTS

FREE DOWNLOAD

https://aipea.org/aes-books/

INTERNATIONAL CLAY CONFERENCES
aipea

XVII ICC
ISTANBUL 2022
25 -29 JULY

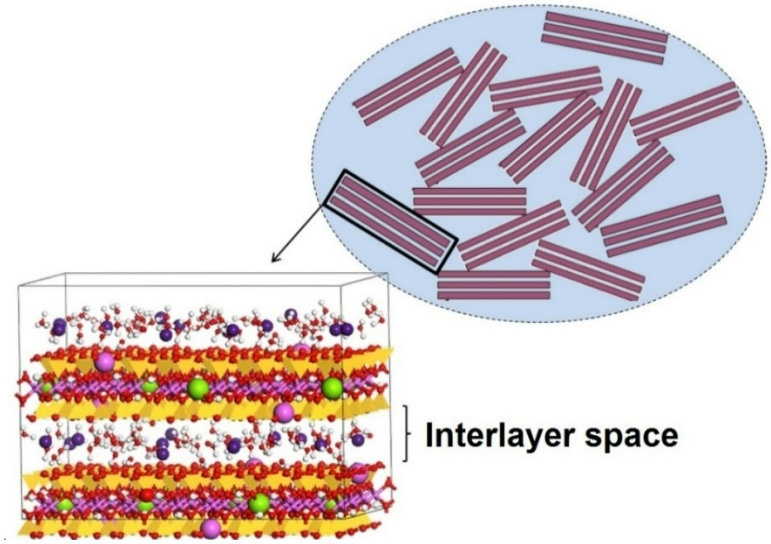

Thematic Session 28

Multiscale computational modeling of clay-related materials and their fluid interfaces

Andrey G. Kalinichev
Directeur de Recherche, SUBATECH (UMR 6457 - IMT Atlantique, Université de Nantes (CNRS/IN2P3), Nantes, France
kalinich@subatech.in2p3.fr

Thomas R. Underwood
Postdoctoral Research Associate, Civil & Environmental Engineering-Princeton University (E-208 E-Quad), Princeton, NJ, 08544, USA
thomas.underwood@princeton.edu

A special issue of the journal ***Clays and Clay Minerals*** is planned on the basis of this session

Acknowledgments

Grand Equipment National de Calcul Intensif

Partnership for Advanced Computing in Europe (PRACE)

IMT Atlantique - Industrial Chair
"Storage and Disposal of Radioactive Waste"

US Department of Energy, Basic Energy Sciences Program, Division of Geosciences

US DOE National Energy Research Scientific Computing Center